

Cosmic history of integrated galactic stellar initial mass function : a simulation study

Tanuka Chattopadhyay¹, Tuli De² and Asis.Kumar.Chattopadhyay³

¹ Department of Applied Mathematics, University of Calcutta, 92 A.P.C Road, Kolkata 700009, India; tanuka@iucaa.ernet.in

² Department of Oncology, Novartis Health Care Pvt. Ltd., Hyderabad, India; tuli.de@novartis.com

³ Department of Statistics, University of Calcutta, 35 B.C Road, Kolkata 700019, India; akestat@caluniv.ac.in

ABSTRACT

Theoretical as well as observational studies suggest that the stellar initial mass function (IMF) might become top heavy with increasing redshift. Embedded cluster mass function is a power law having index β , whose value still remains controversial. In the present work, we investigate the effect of evolving IMF and varying indices of β for the integrated galactic initial mass function, in relation to several measures of star formation rates of galaxies at various redshifts by random simulation. The resulting IGIMF is segmented power law at various redshifts having slopes $\alpha_{1,IGIMF}$ and $\alpha_{2,IGIMF}$ with a turnover at a characteristic mass m_c' . These differ from the stellar initial mass functions with slopes $\alpha_{1,IMF}$, $\alpha_{2,IMF}$, and characteristic masses m_c for different values of redshift z , β , minimum and maximum masses of the embedded clusters.

Key words: galaxies: star clusters: general - galaxies: evolution

1 INTRODUCTION

The form of stellar initial mass function is of considerable debate in the present era as it describes the nature of stellar population, the ratio of high mass to low mass stars and influences the dynamical evolution of star clusters as well as star formation history of the whole galaxy. Usually it is derived using observed luminosity function together with an assumed mass-to-light ratio for the stars under consideration. Generally, IMFs, as suggested by various authors, are either of Salpeter type (Salpeter 1955) or consists of segmented power laws (Scalo 1986; Kroupa 2001; Chabrier 2003) with a turnover at some characteristic mass m_c . The power law slope at high masses is probably close to the Salpeter value (Salpeter 1955) with $\frac{dN}{dm} \propto m^{-\alpha}$, $\alpha = 2.35$ with an uncertainty ~ 0.3 (Chabrier 2003). The form of IMF at present time is more or less Universal (there are evidences of mass segregation to some extent in young massive clouds (Zwart et al. 2010 and references there in) and some variations in star burst galaxies (Gunawardhana et al. 2011)) compared to bottom heavy IMF in massive ellipticals (Ferreras et al. 2013) and there is no direct evidence for rapid variation of IMF within Milky Way disc (Kroupa 2001; Chabrier 2003). This does not exclude the possibility of variation of IMF with time (hence redshift), metallicity or environment. In a work Larson (Larson 2003; Larson 2005) has argued that the characteristic mass is primarily determined by Jeans mass which depends on

the temperature. Hence, with the increase of temperature (cosmic microwave background temperature was higher at higher redshift), one might expect that low mass star formation is disfavored resulting in a top heavy IMF with a temperature scaling with redshift as $(1+z)^{\frac{3}{2}}$. Therefore at sufficiently high redshift, mass scales as $(1+z)^{\frac{3}{2}}$, increasing the fraction of high mass stars. Larson (2005) has suggested that at $z = 5$ the characteristic mass may be higher than present day's value by an order of magnitude.

Recently from various observations it is clear that stars form in embedded clusters (Lada & Lada 2003; Kroupa et al. 2005). These clusters also follow a mass function which is again a power law, $\xi_{ecl}(M) \propto M_{ecl}^{-\beta}$. This is known as embedded cluster mass function (hereafter ECMF). The maximum mass of the ECMF, $M_{ecl,max}$ has been found to depend on the star formation rate of the galaxy (Weidner & Kroupa 2004; Bastian 2008) and is given as

$$M_{ecl,max} = 8.5 \times 10^4 \times SFR^{0.75} \quad (1)$$

Weidner et al. (2013) have suggested a time dependent IMF for elliptical galaxies to account for an excess of low mass stars in these galaxies. They modeled the SFR as a function of time. The SFR reaches a maximum initially and then asymptotically reduces to zero with time. Similar trend of SFR has also been found for various elliptical galaxies as a function of redshift (Spaans & Carollo 1997). Various theoretical models for star formation are difficult to testify

as current observational result from cosmological studies do not measure IMF slopes and SFRs for individual galaxy but study indirect evidence for whole populations and average the results over the galaxy luminosity function.

Smit et al. (2012) have computed the SFR function which is a Schechter function (Schechter 1976), using a characteristic SFR parameter denoted by SFR^* . In their work SFR^* values are calculated for $z \sim 0 - 8$, using ultra violet (UV) luminosity function parameters from Bouwens et al. (2007, 2011), and are compared with similar parameters calculated by various authors (Reddy & Steidel 2009; Reddy et al. 2008; Bell et al. 2007; Magnelli et al. 2011; Sobral et al. 2012).

In the present problem we have replaced the SFR in equation (1) by several significant measures of SFR, e.g. SFR_1 , SFR_2 , SFR_3 and SFR^* which correspond to the first, second, third quartiles and characteristic value of \log_{10} SFR distribution computed by Smit et al. (2012). The first three measures have been computed from the normalized \log_{10} SFR distribution (Smit et al. 2012) as a function of z and the last one is given in Smit et al. (2012) as a function of z . All the four values satisfy tapered power law function (viz. subsection 2.1). As a result $M_{ecl,max}$ becomes a function of z in all four cases. The significance for the use of the above three quartiles and characteristic star formation rate and their derivation have been discussed in detail in sub section 2.1.

In the work by Chattopadhyay et al. (2011), the authors have considered the random fragmentation of young massive clouds in our Galaxy as well as in external galaxies. There they found no correlation between the maximum mass of a star to its embedded cluster mass. Existence of a correlation between the above two affects the star formation history of the cloud. Low mass clouds do not have enough mass to form high mass stars (Bruzual& Charlot 2003; Larson 2006; Weidner et al. 2007; Weidner et al. 2010). Formation of massive stars is possible if they accrete their masses from surrounding. On the other extent, in massive clouds, once the high mass stars are formed, their ionizing radiation removes remaining gas (Weidner et al. 2006). This stops formation of low mass stars. This fact is reflected in some observations (Weidner et al. 2010 and references therein).

In contrast, the recent observations by Maschberger& Clarke (2008) and Parker & Goodwin (2007) included several examples of low mass clusters containing high mass stars. Corbelli et al. (2010) found that for YMCs of M33, such strict correlation does not exist. Moreover unresolved binaries play an important role. Elmegreen (2006) argued that clusters are built stochastically: the large amount of molecular gas present in the star formation region allows high mass stars to form even in a low SFR region i.e., the entire range of masses ($0.01M_\odot$ to $150M_\odot$) is possible even in a low SFR region. Andrews et al. (2013) studied the dwarf star burst galaxy and found no such correlation between maximum mass of star with cluster mass. Furthermore previous observations included very small numbers of YMCs ($\sim 10^5 - 10^6 M_\odot$) (viz. $\sim 10\%$ Weidner et al. 2013),

for which any such correlation is difficult to predict.

Cerviño et al. (2013) have argued that simulated sampling is not in contradiction of a possible $m_{max} - M_{ecl}$ correlation and it depends on the star formation process and the assumed definition of stellar cluster. Hence considering all aspects, we have not assumed any such correlation but only the scenario that massive clouds have a general tendency to form massive stars and have taken the minimum and maximum mass of fragments to be $0.1M_\odot$ (Hass & Ander 2010) and $150M_\odot$ respectively.

In the present work, we have considered the resulting integrated galactic stellar mass function (IGIMF) as a function of redshift due to random fragmentation of embedded clusters of various masses present in that parent galaxy. Section 2 describes the model with model parameters. Section 3 describes the method. Sections 4 and 5 give results and conclusion.

2 THE MODEL

In the present model, the star formation scenario of a galaxy has been considered. A galaxy consists of molecular clouds of various masses and each cloud, under gravitational instability undergo hierarchical fragmentation (Hoyle 1953) giving rise to a number of fragments of various masses. These fragments ultimately form stars and we get what we call stellar initial mass function of these star clusters embedded into the molecular clouds. For simplicity we have assumed that the IMF, in each parent cloud has the same distributional form and this is a segmented power law of the form

$$\xi_{IMF}(m) = \frac{dN}{dm} = \begin{cases} Am^{-\alpha_{1,IMF}}, & m_{min} \leq m < m_c \\ Bm^{-\alpha_{2,IMF}}, & m_c \leq m < m_{max} \end{cases} \quad (2)$$

where m_{min} and m_{max} are the minimum and maximum masses of the stars, m_c is the characteristic mass at which the turnover occurs. The values of A and B are calculated as follows:

Since ξ_{IMF} is a probability density function, we have the normalization condition,

$$\int_{m_{min}}^{m_{max}} \xi_{IMF}(m) dm = 1 \quad (3)$$

Also the IMF is continuous at m_c . Hence the continuity condition gives $Am_c^{-\alpha_{1,IMF}} = Bm_c^{-\alpha_{2,IMF}}$ i.e.

$$A = Bm_c^{\alpha_{1,IMF} - \alpha_{2,IMF}} \quad (4)$$

Then from equation(3)

$$\int_{m_{min}}^{m_c} Am^{-\alpha_{1,IMF}} dm + \int_{m_c}^{m_{max}} Bm^{-\alpha_{2,IMF}} dm = 1$$

Substituting the value of A from equation (4) we get,

$$B = \frac{1}{\frac{m_c^{\alpha_{1,IMF} - \alpha_{2,IMF}}}{(1 - \alpha_{1,IMF})} (m_c^{1 - \alpha_{1,IMF}} - m_{min}^{1 - \alpha_{1,IMF}}) + \frac{1}{1 - \alpha_{2,IMF}} (m_{max}^{1 - \alpha_{2,IMF}} - m_c^{1 - \alpha_{1,IMF}})} \quad (5)$$

Then using B from equation (5), A is found from equation (4). The representative values of $\alpha_{1,IMF}$ and $\alpha_{2,IMF}$ are chosen as 1.25 (the maximum value is 1.25 in low mass regime, Bastian et al. 2010) and 2.35 (Salpeter 1955) respectively.

The values of m_{min} and m_{max} are chosen as $0.1M_\odot$ and $150M_\odot$ respectively (Zinnecker & York 2007). The value of the characteristic mass at $z = 0$ is taken as $m_c(z = 0) = 0.3M_\odot$ (Larson 2005). Since, we have assumed a top heavy IMF with increasing redshift the characteristic mass

$$m_c = D(1 + z)^{\frac{3}{2}} \quad (6)$$

where D is determined from the condition that at $z = 0$, $m_c = 0.3M_\odot$ (Larson 2005). The choice of the above relation is not arbitrary but has a strong physical ground. The influence of temperature on the Jeans mass (Jeans 1902) is very well known phenomenon. Larson (1998, 2005) has discussed that characteristics turnover mass may be primarily determined by thermal Jeans mass which is strongly influenced by temperature ($\sim T^{3/2}$) at fixed density. Hence it is expected that environment, where heating occurs through far infrared radiation, disfavors formation of low mass stars. Such extreme environments really occur in the super clusters at the centre of Milky Way. Some young super clusters at the centre of M82 really appear to have a top heavy IMF (e.g. Rieke et al. 1993; McCrady et al. 2003) along with those at the centre of our Galaxy (Stolte et al. 2005; Maness et al. 2007). The mass functions in these super clusters also have the additional effects of complex dynamical phenomena which make them top heavy over time (McCrady et al. 2005; Kim et al. 2006; Harayama et al. 2008). At the initial stage of star formation in giant as well as in dwarf galaxies the star formation occurs in 'burst' rather than through a continuous process (Steidel et al. 1996; Blain et al. 1999; Lacey et al. 2008). This means IMF becomes more and more top heavy at redshifts 1 - 3 and beyond. Also at high redshift the metallicity was lower in star forming clouds. Thus initially cooling process was not efficient which may lead to an extremely top heavy IMF for the first generation stars (Abel et al. 2002; Bromm et al. 2002). Hence IMF may depend on redshift. Cosmic microwave background temperature (CMB) plays a significant role for increasing the temperature of the medium which scales as $(1 + z)$. Beyond $z \sim 2$, the CMB temperature exceeds the temperature of the Galactic molecular clouds (Evans et al. 2001; Tafalla et al. 2004). Hence it can be speculated that the characteristic mass $m_c \sim T^{3/2}$ at fixed density, varies with redshift as $(1 + z)^{3/2}$, at high redshift leading to a top heavy IMF (Larson 1998). The effect becomes more pronounced when pressure is taken into account and Larson (2005) has shown that at $z = 5$, m_c becomes higher by an order of magnitude than its present value. The direct evidence of a top heavy IMF at high redshift is very rare though there are few observations e.g.

blue rest frame ultra violet colours of galaxies at $z \sim 6$ may imply a top heavy IMF (Stanway et al. 2005). Tumlinson (2007) finds that the properties of carbon enhanced metal poor stars in our Galaxy are best explained by relatively large number of stars in the mass range 1 - 8 M_\odot at high redshift.

The maximum mass of the embedded cluster $M_{ecl,max}$ has been assumed as a function of redshift as discussed in Section 1 and equation (1). The ECMF is assumed as

$$\xi_{ecl}(M) = \frac{dN}{dM_{ecl}} = EM_{ecl}^{-\beta}, M_{ecl,min} \leq M_{ecl} \leq M_{ecl,max} \quad (7)$$

where $M_{ecl,min}$ is the minimum mass of embedded cluster. The value of index β is around 2 (Zhang & Fall 1999; de Grijs et al. 2003; McCrady & Graham 2007). Some studies also suggest flatter slopes like 1.8 (Dowell et al. 2008). The mass spectrum of giant molecular clouds shows, $\beta \sim 1.7$ (Rosolowsky 2005). In the present work we have considered β ranging from 2 to 2.6. The lower limit of embedded cluster is considered as a parameter having values 500 and 1000 M_\odot respectively. The value of the constant E in equation (7) is determined assuming a galaxy mass of $5 \times 10^{11} M_\odot$, whose 30 percent mass has been exhausted due to star formation (Lada et al. 1984; Elmegreen & Clemens 1985; Verschueren et al. 1982). i.e.,

$$0.3 \times 5 \times 10^{11} = \int_{M_{ecl,min}}^{M_{ecl,max}} M_{ecl} \xi_{ecl}(M) dM_{ecl} \quad (8)$$

Then the integrated galactic initial mass function (hereafter IGIMF) as a function of fragment mass m and redshift z, is the collection of all IMFs of all the parent clusters (Kroupa & Weidner 2003; Weidner & Kroupa 2005; Vanbeveren 1982) which is,

$$\xi_{IGIMF}(m, z) = \int_{M_{ecl,min}}^{M_{ecl,max}} \xi_{IMF}(m) \xi_{ecl}(M) dM_{ecl} \quad (9)$$

All the values of the parameters considered are listed in Table 1.

2.1 Various measures of star formation rate

To compute various measures of SFR as a function of redshift (z) we start with the star formation rate function $\phi(SFR)$ derived by Smit et al.(2012) which is,

$$\phi(SFR)dSFR = \phi_{SFR}^* \left(\frac{SFR}{SFR^*} \right)^{\alpha_{SFR}} \exp\left(-\frac{SFR}{SFR^*}\right) \frac{dSFR}{SFR^*} \quad (10)$$

Where ϕ_{SFR}^* , α_{SFR} and SFR^* are various Schechter parameters given as a function of z in Tables 2 and 3 of Smit et al. (2012).

Then $\log_{10}\phi(SFR)$ function is,

$$\log_{10}\phi(SFR) \quad d\log_{10}SFR = [\log_{10}(\phi_{SFR}^*) + \alpha_{SFR} \log_{10}(\frac{SFR}{SFR^*}) -$$

$$\frac{SFR}{SFR^*} \log_{10}e - \log_{10}SFR^*] d\log_{10}SFR \quad (11)$$

At first step we convert $\log_{10}\phi(\text{SFR})$ to a density function at each z dividing by ,

$$T = \int_0^{\log_{10}\text{SFR}_{\max}} \log_{10}\phi(\text{SFR}) \, d\log(\text{SFR}),$$

where $\log_{10}\text{SFR}_{\max}$ is the maximum value of $\log_{10}\text{SFR}$ at a particular z, taken from Fig.2 of Smit et al. (2012) for z = 4, 5, 6, 7. For other values of z the values of $\log_{10}\text{SFR}_{\max}$ were found by plotting the function. The lower boundary is not strictly zero and it includes negative values also (Fig. 2 of Smit et al. 2012) but the number of observations for negative values of $\log_{10}\text{SFR}$ decreases and for $z \sim 6, 7$ (viz. Table 1 of Smit et al. 2012) it is just one. So the negative part of $\log_{10}\text{SFR}$ contribution is insignificant compared to positive part on the basis of observational range. Therefore we limited our study of $\log_{10}\text{SFR}$ from 0 to $\log_{10}\text{SFR}_{\max}$ due to lack of observational points for the negative part and we have worked with available observational range.

Then the c.d.f of $\log_{10}\text{SFR}$ distribution is given by

$$\begin{aligned} \frac{1}{T} \int_0^{\log_{10}\text{SFR}} \log_{10}\phi(\text{SFR}) \, d\log_{10}\text{SFR} = \\ \frac{1}{T} \int_0^{\log_{10}\text{SFR}} [\log_{10}(\phi_{\text{SFR}}^* + \alpha_{\text{SFR}} \log_{10}(\frac{\text{SFR}}{\text{SFR}^*})) - \end{aligned} \quad (12)$$

In equation (12) when the LHS is 0.25 then the corresponding value of $\log_{10}\text{SFR}$ is $\log_{10}\text{SFR}_1$ i.e. the first quartile. This is a point such that at this point 75 % of the galaxies have $\log_{10}\text{SFR} > \log_{10}\text{SFR}_1$ and remaining 25 % of the galaxies have $\log_{10}\text{SFR} \leq \log_{10}\text{SFR}_1$ at a particular z. Similarly we have values of $\log_{10}\text{SFR}_1$ for different z for different values of $\log_{10}\phi_{\text{SFR}}^*$, α_{SFR} and $\log_{10}\text{SFR}^*$ at different z given in Tables 2 and 3 of Smit et al. (2012). We fit the values of $\log_{10}\text{SFR}_1$ at different z by a tapered power law function. We repeat the above process for values of c.d.f as 0.5 and 0.75 and we get $\log_{10}\text{SFR}_2$ and $\log_{10}\text{SFR}_3$ as function of z. The fitted tapered power law functions against $\log_{10}\text{SFR}_1$, $\log_{10}\text{SFR}_2$, $\log_{10}\text{SFR}_3$, $\log_{10}\text{SFR}^*$ are shown in Figs 1 - 4 along with their p-values. We have not only fitted tapered power law but also performed the goodness of fit test for which the p-values are much higher (more than 0.25). Hence we can accept the null hypothesis (the tapered power law is a suitable curve). The significance of constructing these quartile points and $\log_{10}\text{SFR}^*$ as function of z is that we will have a clear view how SFR of most of the galaxies vary with redshift. Among all SFR2 is the most representative measure because $\log_{10}\text{SFR}_2$ is the median value of $\log_{10}\text{SFR}$ distribution.

3 METHOD: MONTE CARLO SIMULATION

To generate a sample of embedded cluster masses from power law with a given range of values it can be considered as truncated Pareto distribution. For this we have used the standard method of inverting the cumulative distribution function (cdf). Let X be a random variable with probability density function (pdf) $f(x)$ and cdf $F(x)$, where

$$F(x) = \int_{-\infty}^x f(x) \, dx \quad (13)$$

$$\int_{-\infty}^{\infty} f(x) \, dx = 1$$

We know that the cdf $F(x)$ follows Uniform distribution over the range (0,1). Hence a simulated value x of X can be obtained by solving the equation $F(x) = r$, where r is a random fraction. Thus one simulated value is given by $x = F^{-1}(r)$. Corresponding to n choices of r, we will have n values of x giving a simulated sample of size n. Of course the above method is valid when the inverse function of F exists, which is true in the present case. To generate the value of X, it is necessary to know the parameters of the Pareto distribution and those are the constants in the Power laws already known from physical considerations. In the present work, in equation (7) lower limit of cluster mass is taken as $M_{\text{ecl},\min}$ instead of $-\infty$, with $f(x) = \xi_{\text{ecl}}(M)$ for sampling cluster masses.

The method of generating samples of stellar masses from a segmented power law is as follows:

$$\text{Let, } \xi_{\text{IMF}}(m) = \frac{dN}{dm} = \begin{cases} Am^{-\alpha}; m_{\min} < m \leq m_c \\ Bm^{-\beta}; m_c < m \leq m_{\max} \end{cases} \quad (14)$$

where A and B are constants to be determined by equations (4) and (5). Now, to generate samples from the above power laws, we use a conditional cdf defined as follows:

$$F_1(m) = P(X < m | m_{\min} < x < m_c) = \frac{F(m) - F(m_{\min})}{F(m_c) - F(m_{\min})} \quad m_{\min} < m < m_c. \quad (15)$$

$$\begin{aligned} \text{In the same way,} \\ F_2(m) = P(X < m | m_c < x < m_{\max}) = \frac{F(m) - F(m_c)}{F(m_{\max}) - F(m_c)} \\ m_c < m < m_{\max} \end{aligned} \quad (16)$$

We use the method of inversion to draw samples using these two conditional cdfs. Firstly when $m_{\min} < m < m_c$, we draw a random sample say u_1 from a Uniform distribution, i.e., $U(0,1)$ and equate it to

$$F_1(m) = \frac{F(m) - F(m_{\min})}{F(m_c) - F(m_{\min})} = u_1 \quad (17)$$

So that inverting it we get the expression for the sample m as

$$m = [u_1 \times (m_c^{(1-\alpha)} - m_{\min}^{(1-\alpha)}) + m_{\min}^{(1-\alpha)}]^{\frac{1}{(1-\alpha)}} \quad (18)$$

Thus when $u_1 = 0$, $m = m_{\min}$ and when $u_1 = 1$, $m = m_c$. Similarly, when $m_c < m < m_{\max}$, we draw a random sample say u_2 from a Uniform distribution, i.e., $U(0,1)$ and equate it to

$$F_2(m) = \frac{F(m) - F(m_c)}{F(m_{\max}) - F(m_c)} = u_2 \quad (19)$$

So that inverting it we get the expression for the sample m as

$$m = [u_2 \times (m_{\max}^{(1-\beta)} - m_c^{(1-\beta)}) + m_c^{(1-\beta)}]^{\frac{1}{(1-\beta)}} \quad (20)$$

Thus when $u_2 = 0, m = m_c$ and when $u_2 = 1, m = m_{max}$.

We simulate from $F_1(m)$ as long as the total mass of the embedded cluster is equal to the mass in the low mass regime (viz $m_{min} < m < m_c$) and then we simulate from $F_2(m)$ for the high mass regime (viz. $m_c < m < m_{max}$). The mass fractions for each embedded cluster in the low and high mass regimes are computed at the beginning for different m_c s. In the present work we have simulated random samples from various truncated power law and segmented power law distributions as follows.

(i) First we simulate a sample of embedded cluster masses following the normalized power law given in equation (7), where the maximum mass is computed at any particular z following equation (1) for different SFR (viz. SFR1, SFR2, SFR3 and SFR*). The simulation is continued as long as the total mass of the parent clouds is less or equal to 30 percent of the total mass of the galaxy.

(ii) Secondly for each mass of a parent cluster we simulate a sample of stellar masses following the segmented power law (as discussed before) distributions, given in equation (2) at a particular value of z , so that the value of the characteristic mass, m_c is prefixed at that value of z (refer to equation (6)). Each time a stellar mass is simulated, the total mass of the previous stellar masses is checked with the total mass of the embedded cluster and as soon as it exceeds the mass of the parent cluster, the simulation is stopped.

(iii) Finally the mass spectrum of all simulated fragment masses from all the parent clusters of the galaxy is computed and fitted by segmented power laws, to give the resulting form of the IGIMF.

(iv) The above procedure is performed at various SFR (viz. SFR1, SFR2, SFR3, SFR*), redshifts z , $M_{ecl,min}$ and β respectively.

4 RESULTS AND INTERPRETATION

Tables 2 - 5 and Figs. 5 - 16 show the resulting IGIMF slopes, for stars in a galaxy which consists of segmented power laws with slopes, $\alpha_{1,IGIMF}$ in low mass regime and $\alpha_{2,IGIMF}$ in high mass regime for various values of SFR, β , $M_{ecl,min}$ and redshift $z = 0.1$ to $z = 6.8$ respectively. The following observations are envisaged.

(i) As z increases, $\alpha_{2,IGIMF}$ becomes systematically rising up to $z \sim 2$ and then starts falling. It is again rising from around $z \sim 4$ and runs down around $z \sim 6$. The effect is more pronounced for $\beta = 2$ and 2.4. For $\beta = 2.6$ the rise and fall are comparatively small (viz. Figs.5 - 7). This might be explained as follows. Though from $z = 0 - 2$ the SFR and hence $M_{ecl,max}$ are increasing (viz. equation 1), due to low temperature of the ambient medium Jeans mass does not favor formation of massive stars. That is why $\alpha_{2,IGIMF}$ is taking higher values i.e. steeper slopes for $z = 0 - 2$. But gradually due to the rise of temperature of the medium with increasing z , formation of massive stars predominates even for a comparatively lower but still moderate SFR and hence

for moderate $M_{ecl,max}$. This favors formation of massive stars which makes $\alpha_{2,IGIMF}$ lower for $z \sim 2 - 4$. The effect becomes reduced due to rapid fall of SFR at very high z (viz. $z \sim 4 - 6$, Figs. 1 - 4) increasing $\alpha_{2,IGIMF}$ indices again.

(ii) As β increases, changes in the rising and falling of $\alpha_{2,IGIMF}$ become faster. The effect is very pronounced for $\beta \sim 2 - 2.4$. This is because, as β increases, the number of low mass clusters become higher compared to the number of high mass clusters. So the above mentioned effect becomes accentuated due to steepening of the mass function of embedded clusters (Fig. 6).

(iii) $\alpha_{2,IGIMF}$ becomes flatter as $M_{ecl,min}$ increases when β is low. This is because when β is low, number of low mass clusters decreases and as a result massive star formation is favored compared to low mass stars. This results in the flattening of the slopes, $\alpha_{2,IGIMF}$ in high mass regime. For higher values of β (> 2), number of low mass clusters increases which disfavors formation of massive stars and $\alpha_{2,IGIMF}$ becomes steeper as a result.

(iv) $\alpha_{2,IGIMF}$ is always flatter than the IMF slopes. This might be the joint effect of various star formation rates as well as increasing temperature of the environment with increasing redshifts. Up to $z \sim 2$ the temperature of the ambient medium is lower compared to the higher redshift zone. Hence Jeans masses are lower. But at the same time SFR is increasing to its maximum increasing $M_{ecl,max}$ which favors over all formation of massive stars compared to IMF. On the other hand for $z > 2$, Jeans masses are higher and SFR gradually decrease lowering values of $M_{ecl,max}$, hence increasing low mass stars. Somehow the joint effect of these two phenomena is responsible for a resulting flatness of $\alpha_{2,IGIMF}$. This is consistent with some observational results (Alonso et al. 2004; Finoguenov et al. 2003; Lowenstein 2006; Nayakshin & Sunyaev 2005) which indicate IGIMF to be top heavy (i.e. massive stars form in large numbers compared to less massive stars) when $SFR \geq 100 M_\odot yr^{-1}$. The above trend is also in good agreement for Galactic and M31 bulge (Ballero et al. 2007) as well as Wilkin et al. (2011) for present day mass density from cosmological star formation history. The trend for decreasing slope with increasing SFR has also been found by Gunawardhana et al. (2011) for a sample of 40000 galaxies. For $z > 2$, though the SFR decreases and formation of massive clouds are not favored, but still massive stars are produced in some optimum zone due to the increase in temperature of the medium so that m'_c is shifted towards higher mass (i.e. a top heavy mass spectrum with steeper slope) (viz. Figs.9 - 16).

(v) The characteristic mass m_c of stellar initial mass function differs from characteristic mass, m'_c , of integrated galactic mass function. Generally $m_c \geq m'_c$.

(vi) the above mentioned effects are similar for various measures of SFR though there are small variations. The measure SFR1 is the first quartile i.e. 25 % of the galaxies have $SFR \leq SFR1$ and 75% of the galaxies have $SFR > SFR1$ i.e. we can say SFR1 is representative one for low SFR which is the characteristics of dwarf galaxies. On the other hand

SFR3 is representative one of high SFR which characterizes giant galaxies. In this regard SFR2 is the measure of average SFR of galaxies. Now in dwarf galaxies due to its low SFR, formation of massive stars are not favorable in large numbers. Thus it is most likely that $\alpha_{2,IGIMF}$ for SFR1 is rather steeper than that of $\alpha_{2,IGIMF}$ for SFR2 followed by $\alpha_{2,IGIMF}$ for SFR3. It is clear from Tables 2 - 4 that $\alpha_{2,IGIMF}$ for SFR1 > $\alpha_{2,IGIMF}$ for SFR2 in 72 % - 78 % cases for $\beta = 2 - 2.6$ and $\alpha_{2,IGIMF}$ for SFR2 > $\alpha_{2,IGIMF}$ for SFR3 in 50 % - 60 % cases for $\beta = 2 - 2.6$. SFR* is the point of the SFR function where the function levels off from exponential to a shallower power law i.e. from this point the SFR does not vary much to the left i.e. for low SFR. So SFR* is sort of representative value of low SFR i.e. of less massive galaxies. $\alpha_{2,IGIMF}$ for SFR* > $\alpha_{2,IGIMF}$ for SFR2 in 67% - 50 % cases for $\beta = 2 - 2.6$. Therefore SFR1/ SFR*, SFR2, SFR3 might be representative star formation histories for dwarf, intermediate and giant galaxies.

5 CONCLUSION

In the present work the nature of observed star formation rate has been investigated (viz. SFR1, SFR2, SFR3 and SFR*) as a function of redshift instead of empirical SFR, for various galaxies together with a top heavy stellar IMF whose characteristic mass increases with redshift. This helps to study the cosmic star formation history in galaxies. A Monte Carlo simulation method is used to find the IGIMF. It is found that the high mass slope of the galactic mass function becomes a function of star formation rate, temperature of the medium and cluster mass function. Up to a redshift of $z \sim 2$, the galactic mass function becomes steeper compared to a flatter one for $z > 2$ followed again by a steeper one around $z \sim 6$. This is due to the joint effect of SFR and temperature of the ambient medium. The galactic mass function is affected by the embedded cluster mass-spectrum . It is also influenced by the minimum mass of the parent cluster.

6 ACKNOWLEDGEMENT

The authors are very grateful to referee for giving important and useful suggestions for improving the quality of the work to a great extent.

REFERENCES

- Abel, T., Bryan, G. L., & Norman, M. L. 2002, Science, 295, 93
- Alonso-Herrero, A., Takagé, T., Baker, A.J. et al. 2004, ApJ, 612, 222.
- Andrews, J.E., Calzetti, D., Chandar, R., Lee, J.C., Elmegreen, B.G., Kennicutt, R.C., Whitmore, B., Kissel, J.S., daSilva, R.L., Krumholz, M.R., O'Connell, R.W., Dopita, M.A., Frogel, J.A., & Kim H. 2013, ApJ, 767, 51.
- Ballero, S.K., Matteucci, F., Origlia, L., Rich, R.M. 2007, A&A, 467, 123.
- Bastian, N., Covey, K.R. & Meyer, M.R. 2010, ARA&A, 48, 339.
- Bastian, N. 2008, MNRAS, 390, 759.
- Bell, E.F., Xheng, X.Z., Papovich, C., Borch, A., Wolf, C., Meisenheimer, K. 2007, ApJ, 663, 834.
- Blain, A. W., Jameson, A., Smail, I., Longair, M. S., Kneib, J.P., & Ivison, R. J. 1999, MNRAS, 309, 715.
- Bouwens, R.J., Illingworth, G.D., Franx, M., Ford, H. 2007, ApJ, 670, 928.
- Bouwens, R.J., Illingworth, G.D., Oesch, P.A., Labb, I., Trenti, M., van Dokkum, P., Franx, M., Stiavelli, M., Carollo, C.M., Magee, D., Gonzalez, V. 2011, ApJ, 737, 90.
- Bromm, V., Coppi, P. S., & Larson, R. B. 2002, ApJ, 564, 23
- Bruzual, G., Charlot, S. 2003, MNRAS, 344, 1000.
- Cerviño, M., Román-Zúñiga, C., Luridiana, V., Bayo, A., Sánchez, N., Pérez, E. 2013, A & A, 553, 31.
- Chabrier, G. 2003, PASP, 115, 763.
- Chattopadhyay, T., Sinha, A., Chattopadhyay, A.K. 2011, ApJ, 736, 152.
- Corbelli, E., Lorenzoni, S., Walterbos, R.A.M., Braun, R., Thilker, D.A. 2010, A&A, 511, A89.
- de Grij, R., Anders, P., Bastian, N., et al. 2003, MNRAS, 343, 1285.
- Dowell, J.D., Buckalew, B.A., Tan, J.C. 2008, AJ, 2008, 135, 823.
- Elmegreen, B.G., Clemens, C. 1985, ApJ, 294, 523.
- Elmegreen, B.G. 2006, ApJ, 648, 572.
- Evans, N. J., II, Rawlings, J. M. C., Shirley, Y. L., & Mundy, L. G. 2001, ApJ, 557, 193
- Ferreras, I., Cropper, M., Kawata, D., Page, M., Hoversten, E.A. 2013, MNRAS, 424, 1636.
- Finoguenov, A., Burkert, A., Böhringer, H. 2003, ApJ, 594, 136.
- Gunawardhana, M.L.P., Hopkins, A.M., Sharp, R.G. et al. 2011, MNRAS, 415, 1647.
- Hass, M.R., Ander, P. 2010, A & A, 512, A79.
- Harayama, Y., Eisenhauer, F., & Martins, F. 2008, ApJ, 675, 1319.
- Hoyle, F. 1953, ApJ, 118, 513.
- Jeans, J.H. 1902, Phil. Trans. Roy. Soc. A199, 1.
- Kim, S. S., Figer, D. F., Kudritzki, R. P., & Najarro, F. 2006, ApJ, 653, L113
- Kroupa, P. 2001, MNRAS, 322, 231.
- Kroupa, P., Weidner, C. 2003, ApJ, 598, 1076.
- Kroupa, P., Gaia ed, C., Turon, K.S., O'Flaherty Perryman, M.A.C., 2005, ESA.SP, 576.
- Lacey, C. G., Baugh, C. M., Frenk, C. S., Silva, L., Granato, G. L., & Bressan, A. 2008, MNRAS, 385, 1155.
- Lada, C.J., Lada, E.A. 2003, 41, 57.
- Lada, C. J., Margulis, M., & Dearborn, D. 1984, ApJ, 285, 141.
- Larson, R.B. 2003, MNRAS, 301, 569.
- Larson, R.B. 2005, MNRAS, 359, 211.
- Larson, R.B. 2006, 26, 55.
- Larson, R.B. 1998, MNRAS, 301, 569.
- Loewenstein, M. 2006, ApJ, 648, 230.
- Magnelli, B., Elbaz, D., Chary, R.R., Dickinson, M., Le Borgne, D., Frayer, D.T., Willmer, C.N.A. 2011, A&A, 528, A35.
- Maschberger, T., Clarke, C.J. 2008, MNRAS, 391, 711.
- Maness, H., et al. 2007, ApJ, 669, 1024.
- McCrady, N. & Graham, J. R. 2007, ApJ, 663, 844.
- McCrady, N., Graham, J. R., & Vacca, W. D. 2005, ApJ, 621, 278.

- McCrady, N., Gilbert, A. M., & Graham, J. R. 2003, ApJ, 596, 240.
- Nayakshin, S., Sunyaev, R. 2005, MNRAS, 364, L23.
- Parker, R.J., Goodwins, S.P. 2007, MNRAS, 380, 1271.
- Reddy, N.A., Steidel, C.C., Pettini, M., Adelberger, K.L., Shapley, A.E., Erb,D.K., Dickinson, M. 2008, ApJS, 175, 48.
- Reddy, N.A., Steidel, C.C. 2009, ApJ, 692, 778.
- Rieke, G. H., Loken, K., Rieke, M. J., & Tamblyn, P. 1993, ApJ, 412, 99
- Rosolowsky, E. 2005, PASP, 117, 1403.
- Salpeter, E.E. 1955, ApJ, 121, 161.
- Scalo, J.M. 1986, Fundam.Cosm.Phys, 11, 1.
- Schechter, P. 1976, ApJ, 203, 297.
- Sobral, D., Smail, L., Best, P.N., Geach, J.E., Matsuda, Y., Stott, J.P., Cirasuolo, M., Kurk ,J. 2012, MNRAS.(in press) (arXiv:1202.3436).
- Smit, R., Bouwens, R.J., Franx, M. , Illingworth, G.D., Labbè I, Oesch, A.P., van Dokkum, P.G. 2012, ApJ, 756, 14.
- Spaans, M., Carollo, C.M. 1997, ApJL, 482, L93.
- Stanway, E.R., McMahon, R.G., Bunker, A.J. 2005, MNRAS, 359, 1184.
- Steidel, C. C., Giavalisco, M., Pettini, M., Dickinson, M., & Adelberger, K. L. 1996, ApJ, 462, L17
- Stolte, A., Brandner, W., Grebel, E. K., Lenzen, R., & Lagrange, A.-M. 2005, ApJ, 628, L113.
- Tafalla, M., Myers, P. C., Caselli, P., & Walmsley, C. M. 2004, A&A, 416, 191.
- Tumlinson, J. 2007, ApJ, 664, L63.
- Vanbeveren,D.1982, A&A, 115,65.
- Verschueren, W., Hensberge, H. 1982, A&A, 240, 216.
- Weidner, C., Kroupa, P. 2004, MNRAS, 348, 187.
- Weidner, C., Kroupa, P. 2005, ApJ, 625, 754.
- Weidner, C., Kroupa, P. 2006, MNRAS, 365, 1333.
- Weidner, C., Kroupa, P., Nürnberg, D.E.A., Sterzik, M.F. 2007, MNRAS, 376, 1879.
- Weidner, C., Kroupa, P., Bonnell, .IA.D., 2010, MNRAS, 401, 275.
- Weidner, C., Ferreras, I., Vazdekis, A., Barbera, F. 2013, MNRAS, 435, 2274.
- Wilkin, S.M., Bunker, A.J., Stanway, E., Lorenzoni, S., Caruana, J.2011, A & A, 417, 717.
- Zhang, Q. & Fall, S. M. 1999, ApJ, 527, L81.
- Zinnecker, H., Yorke, H.W. 2007, A&A, 45, 481.
- Zwart, S.F.P., McMillan, S.L.W., Gieles, M. 2010, ARA&A, 48, 431.

Table 1. Initial values of the parameters

Parameter	value
$\alpha_{1,IMF}(z = 0)$	1.25
$\alpha_{2,IMF}(z = 0)$	2.35
Galaxy mass	$5 \times 10^{11} (M_\odot)$
m_{min}	$0.1 M_\odot$
m_{max}	$150 M_\odot$
$m_{c,IMF}(z = 0)$	$0.3 M_\odot$
$M_{ecl,min}$	500,1000(M_\odot)
β	2.0,2.4,2.6
z	0.1,0.2,0.8,1.5,2.2,3.8,5.0,5.9,6.8
efficiency	30%

Table 2. IGIMF and IMF slopes with varying z and $M_{cl,min}$ at $\beta=2, 2.4$ and 2.6 for SFR1:

$\beta = 2.0$													
		$z = 0.1$						$z = 0.2$					
$M_{cl,min}$	$\alpha_{1,IMF}$	$\alpha_{2,IMF}$	m_c	$\alpha_{1,IGIMF}$	$\alpha_{2,IGIMF}$	m_c'	$\alpha_{1,IMF}$	$\alpha_{2,IMF}$	m_c	$\alpha_{1,IGIMF}$	$\alpha_{2,IGIMF}$	m_c'	
500	1.25	2.35	0.381	-0.05	1.475	0.224	1.25	2.35	0.434	0.161	1.367	0.282	
1000	1.25	2.35	0.381	0.072	1.431	0.178	1.25	2.35	0.434	-0.303	1.315	0.282	
$z = 0.8$													
$M_{cl,min}$	$\alpha_{1,IMF}$	$\alpha_{2,IMF}$	m_c	$\alpha_{1,IGIMF}$	$\alpha_{2,IGIMF}$	m_c'	$\alpha_{1,IMF}$	$\alpha_{2,IMF}$	m_c	$\alpha_{1,IGIMF}$	$\alpha_{2,IGIMF}$	m_c'	
500	1.25	2.35	0.797	0.235	1.415	0.562	1.25	2.35	1.304	0.178	1.492	0.891	
1000	1.25	2.35	0.797	0.305	1.404	0.355	1.25	2.35	1.304	0.095	1.384	0.891	
$z = 2.2$													
$M_{cl,min}$	$\alpha_{1,IMF}$	$\alpha_{2,IMF}$	m_c	$\alpha_{1,IGIMF}$	$\alpha_{2,IGIMF}$	m_c'	$\alpha_{1,IMF}$	$\alpha_{2,IMF}$	m_c	$\alpha_{1,IGIMF}$	$\alpha_{2,IGIMF}$	m_c'	
500	1.25	2.35	1.889	0.315	1.555	1.412	1.25	2.35	3.471	0.168	1.358	2.239	
1000	1.25	2.35	1.889	0.224	1.528	1.122	1.25	2.35	3.471	0.505	1.293	2.239	
$z = 5.0$													
$M_{cl,min}$	$\alpha_{1,IMF}$	$\alpha_{2,IMF}$	m_c	$\alpha_{1,IGIMF}$	$\alpha_{2,IGIMF}$	m_c'	$\alpha_{1,IMF}$	$\alpha_{2,IMF}$	m_c	$\alpha_{1,IGIMF}$	$\alpha_{2,IGIMF}$	m_c'	
500	1.25	2.35	4.849	0.237	1.474	4.467	1.25	2.35	5.981	0.522	1.499	11.22	
1000	1.25	2.35	4.849	0.354	1.211	4.467	1.25	2.35	5.981	0.261	1.416	4.467	
$z = 6.8$													
$M_{cl,min}$	$\alpha_{1,IMF}$	$\alpha_{2,IMF}$	m_c	$\alpha_{1,IGIMF}$	$\alpha_{2,IGIMF}$	m_c'	$\alpha_{1,IMF}$	$\alpha_{2,IMF}$	m_c	$\alpha_{1,IGIMF}$	$\alpha_{2,IGIMF}$	m_c'	
500	1.25	2.35	7.189	0.348	1.409	11.22							
1000	1.25	2.35	7.189	0.312	1.145	7.079							
$\beta = 2.4$													
		$z = 0.1$						$z = 0.2$					
$M_{cl,min}$	$\alpha_{1,IMF}$	$\alpha_{2,IMF}$	m_c	$\alpha_{1,IGIMF}$	$\alpha_{2,IGIMF}$	m_c'	$\alpha_{1,IMF}$	$\alpha_{2,IMF}$	m_c	$\alpha_{1,IGIMF}$	$\alpha_{2,IGIMF}$	m_c'	
500	1.25	2.35	0.381	0.654	1.421	0.224	1.25	2.35	0.434	0.254	1.409	0.282	
1000	1.25	2.35	0.381	0.645	1.535	0.224	1.25	2.35	0.434	0.335	1.462	0.282	
$z = 0.8$													
$M_{cl,min}$	$\alpha_{1,IMF}$	$\alpha_{2,IMF}$	m_c	$\alpha_{1,IGIMF}$	$\alpha_{2,IGIMF}$	m_c'	$\alpha_{1,IMF}$	$\alpha_{2,IMF}$	m_c	$\alpha_{1,IGIMF}$	$\alpha_{2,IGIMF}$	m_c'	
500	1.25	2.35	0.797	0.205	1.359	0.562	1.25	2.35	1.304	0.163	1.362	1.122	
1000	1.25	2.35	0.797	0.226	1.461	0.562	1.25	2.35	1.304	0.204	1.455	0.891	
$z = 2.2$													
$M_{cl,min}$	$\alpha_{1,IMF}$	$\alpha_{2,IMF}$	m_c	$\alpha_{1,IGIMF}$	$\alpha_{2,IGIMF}$	m_c'	$\alpha_{1,IMF}$	$\alpha_{2,IMF}$	m_c	$\alpha_{1,IGIMF}$	$\alpha_{2,IGIMF}$	m_c'	
500	1.25	2.35	1.889	0.255	1.369	1.412	1.25	2.35	3.471	0.344	1.432	2.818	
1000	1.25	2.35	1.889	0.215	1.243	1.412	1.25	2.35	3.471	0.294	1.311	4.467	
$z = 5.0$													
$M_{cl,min}$	$\alpha_{1,IMF}$	$\alpha_{2,IMF}$	m_c	$\alpha_{1,IGIMF}$	$\alpha_{2,IGIMF}$	m_c'	$\alpha_{1,IMF}$	$\alpha_{2,IMF}$	m_c	$\alpha_{1,IGIMF}$	$\alpha_{2,IGIMF}$	m_c'	
500	1.25	2.35	4.849	0.185	1.367	3.548	1.25	2.35	5.981	0.183	1.347	4.467	
1000	1.25	2.35	4.849	0.239	1.531	2.818	1.25	2.35	5.981	0.141	1.443	4.467	
$z = 6.8$													
$M_{cl,min}$	$\alpha_{1,IMF}$	$\alpha_{2,IMF}$	m_c	$\alpha_{1,IGIMF}$	$\alpha_{2,IGIMF}$	m_c'	$\alpha_{1,IMF}$	$\alpha_{2,IMF}$	m_c	$\alpha_{1,IGIMF}$	$\alpha_{2,IGIMF}$	m_c'	
500	1.25	2.35	7.189	0.291	1.312	7.079							
1000	1.25	2.35	7.189	0.249	1.281	7.079							
$\beta = 2.6$													
		$z = 0.1$						$z = 0.2$					
$M_{cl,min}$	$\alpha_{1,IMF}$	$\alpha_{2,IMF}$	m_c	$\alpha_{1,IGIMF}$	$\alpha_{2,IGIMF}$	m_c'	$\alpha_{1,IMF}$	$\alpha_{2,IMF}$	m_c	$\alpha_{1,IGIMF}$	$\alpha_{2,IGIMF}$	m_c'	
500	1.25	2.35	0.381	0.072	1.383	0.224	1.25	2.35	0.434	0.495	1.388	0.282	
1000	1.25	2.35	0.381	0.01	1.477	0.224	1.25	2.35	0.434	0.579	1.493	0.282	
$z = 0.8$													
$M_{cl,min}$	$\alpha_{1,IMF}$	$\alpha_{2,IMF}$	m_c	$\alpha_{1,IGIMF}$	$\alpha_{2,IGIMF}$	m_c'	$\alpha_{1,IMF}$	$\alpha_{2,IMF}$	m_c	$\alpha_{1,IGIMF}$	$\alpha_{2,IGIMF}$	m_c'	
500	1.25	2.35	0.797	0.281	1.388	0.562	1.25	2.35	1.304	0.286	1.392	0.891	
1000	1.25	2.35	0.797	0.083	1.468	0.708	1.25	2.35	1.304	0.424	1.409	0.891	
$z = 2.2$													
$M_{cl,min}$	$\alpha_{1,IMF}$	$\alpha_{2,IMF}$	m_c	$\alpha_{1,IGIMF}$	$\alpha_{2,IGIMF}$	m_c'	$\alpha_{1,IMF}$	$\alpha_{2,IMF}$	m_c	$\alpha_{1,IGIMF}$	$\alpha_{2,IGIMF}$	m_c'	
500	1.25	2.35	1.889	0.242	1.461	1.412	1.25	2.35	3.471	0.319	1.357	2.239	
1000	1.25	2.35	1.889	0.218	1.404	1.778	1.25	2.35	3.471	0.256	1.366	2.818	
$z = 5.0$													
$M_{cl,min}$	$\alpha_{1,IMF}$	$\alpha_{2,IMF}$	m_c	$\alpha_{1,IGIMF}$	$\alpha_{2,IGIMF}$	m_c'	$\alpha_{1,IMF}$	$\alpha_{2,IMF}$	m_c	$\alpha_{1,IGIMF}$	$\alpha_{2,IGIMF}$	m_c'	
500	1.25	2.35	4.849	0.288	1.433	4.467	1.25	2.35	5.981	0.342	1.335	7.079	
1000	1.25	2.35	4.849	0.055	1.386	4.467	1.25	2.35	5.981	0.322	1.421	4.467	
$z = 6.8$													
$M_{cl,min}$	$\alpha_{1,IMF}$	$\alpha_{2,IMF}$	m_c	$\alpha_{1,IGIMF}$	$\alpha_{2,IGIMF}$	m_c'	$\alpha_{1,IMF}$	$\alpha_{2,IMF}$	m_c	$\alpha_{1,IGIMF}$	$\alpha_{2,IGIMF}$	m_c'	
500	1.25	2.35	7.189	0.345	1.423	7.079							
1000	1.25	2.35	7.189	0.324	1.446	7.079							

Table 3. IGIMF and IMF slopes with varying z and $M_{cl,min}$ at
 $\beta=2.4$ and 2.6 for SFR2:

$\beta = 2.0$														
$M_{cl,min}$	$z = 0.1$							$z = 0.2$						
	$\alpha_{1,IMF}$	$\alpha_{2,IMF}$	m_c	$\alpha_{1,IGIMF}$	$\alpha_{2,IGIMF}$	m_c'	$\alpha_{1,IMF}$	$\alpha_{2,IMF}$	m_c	$\alpha_{1,IGIMF}$	$\alpha_{2,IGIMF}$	m_c'		
	500	1.25	2.35	0.381	0.429	1.415	0.224	1.25	2.35	0.434	0.019	1.437	0.282	
1000	1.25	2.35	0.381	0.312	1.321	0.224	1.25	2.35	0.434	-0.054	1.404	0.282		
$z = 0.8$														
$M_{cl,min}$	$\alpha_{1,IMF}$	$\alpha_{2,IMF}$	m_c	$\alpha_{1,IGIMF}$	$\alpha_{2,IGIMF}$	m_c'	$\alpha_{1,IMF}$	$\alpha_{2,IMF}$	m_c	$\alpha_{1,IGIMF}$	$\alpha_{2,IGIMF}$	m_c'		
	500	1.25	2.35	0.797	0.129	1.351	0.562	1.25	2.35	1.304	0.307	1.389	0.891	
	1000	1.25	2.35	0.797	0.293	1.408	0.562	1.25	2.35	1.304	0.073	1.488	0.708	
$z = 2.2$														
$M_{cl,min}$	$\alpha_{1,IMF}$	$\alpha_{2,IMF}$	m_c	$\alpha_{1,IGIMF}$	$\alpha_{2,IGIMF}$	m_c'	$\alpha_{1,IMF}$	$\alpha_{2,IMF}$	m_c	$\alpha_{1,IGIMF}$	$\alpha_{2,IGIMF}$	m_c'		
	500	1.25	2.35	1.889	0.129	1.364	1.122	1.25	2.35	3.471	0.449	1.174	2.818	
	1000	1.25	2.35	1.889	0.046	1.245	1.412	1.25	2.35	3.471	0.099	1.214	1.778	
$z = 5.0$														
$M_{cl,min}$	$\alpha_{1,IMF}$	$\alpha_{2,IMF}$	m_c	$\alpha_{1,IGIMF}$	$\alpha_{2,IGIMF}$	m_c'	$\alpha_{1,IMF}$	$\alpha_{2,IMF}$	m_c	$\alpha_{1,IGIMF}$	$\alpha_{2,IGIMF}$	m_c'		
	500	1.25	2.35	4.849	0.249	1.351	3.548	1.25	2.35	5.981	0.323	1.398	7.079	
	1000	1.25	2.35	4.849	0.348	1.298	3.548	1.25	2.35	5.981	0.137	1.392	5.623	
$z = 6.8$														
$M_{cl,min}$	$\alpha_{1,IMF}$	$\alpha_{2,IMF}$	m_c	$\alpha_{1,IGIMF}$	$\alpha_{2,IGIMF}$	m_c'	$\alpha_{1,IMF}$	$\alpha_{2,IMF}$	m_c	$\alpha_{1,IGIMF}$	$\alpha_{2,IGIMF}$	m_c'		
	500	1.25	2.35	7.189	0.241	1.202	7.079							
	1000	1.25	2.35	7.189	0.377	1.223	7.079							
$\beta = 2.4$														
$M_{cl,min}$	$\alpha_{1,IMF}$	$\alpha_{2,IMF}$	m_c	$\alpha_{1,IGIMF}$	$\alpha_{2,IGIMF}$	m_c'	$\alpha_{1,IMF}$	$\alpha_{2,IMF}$	m_c	$\alpha_{1,IGIMF}$	$\alpha_{2,IGIMF}$	m_c'		
	500	1.25	2.35	0.381	0.306	1.404	0.224	1.25	2.35	0.434	0.150	1.358	0.282	
	1000	1.25	2.35	0.381	0.286	1.448	0.282	1.25	2.35	0.434	0.235	1.321	0.282	
$z = 0.8$														
$M_{cl,min}$	$\alpha_{1,IMF}$	$\alpha_{2,IMF}$	m_c	$\alpha_{1,IGIMF}$	$\alpha_{2,IGIMF}$	m_c'	$\alpha_{1,IMF}$	$\alpha_{2,IMF}$	m_c	$\alpha_{1,IGIMF}$	$\alpha_{2,IGIMF}$	m_c'		
	500	1.25	2.35	0.797	0.307	1.400	0.562	1.25	2.35	1.304	0.184	1.378	0.891	
	1000	1.25	2.35	0.797	0.379	1.446	0.562	1.25	2.35	1.304	0.170	1.432	0.891	
$z = 2.2$														
$M_{cl,min}$	$\alpha_{1,IMF}$	$\alpha_{2,IMF}$	m_c	$\alpha_{1,IGIMF}$	$\alpha_{2,IGIMF}$	m_c'	$\alpha_{1,IMF}$	$\alpha_{2,IMF}$	m_c	$\alpha_{1,IGIMF}$	$\alpha_{2,IGIMF}$	m_c'		
	500	1.25	2.35	1.889	0.383	1.365	1.778	1.25	2.35	3.471	0.186	1.351	2.818	
	1000	1.25	2.35	1.889	0.253	1.392	1.412	1.25	2.35	3.471	0.027	1.264	2.238	
$z = 5.0$														
$M_{cl,min}$	$\alpha_{1,IMF}$	$\alpha_{2,IMF}$	m_c	$\alpha_{1,IGIMF}$	$\alpha_{2,IGIMF}$	m_c'	$\alpha_{1,IMF}$	$\alpha_{2,IMF}$	m_c	$\alpha_{1,IGIMF}$	$\alpha_{2,IGIMF}$	m_c'		
	500	1.25	2.35	4.849	0.304	1.420	3.548	1.25	2.35	5.981	0.335	1.333	5.623	
	1000	1.25	2.35	4.849	0.167	1.425	5.623	1.25	2.35	5.981	0.313	1.495	5.623	
$z = 6.8$														
$M_{cl,min}$	$\alpha_{1,IMF}$	$\alpha_{2,IMF}$	m_c	$\alpha_{1,IGIMF}$	$\alpha_{2,IGIMF}$	m_c'	$\alpha_{1,IMF}$	$\alpha_{2,IMF}$	m_c	$\alpha_{1,IGIMF}$	$\alpha_{2,IGIMF}$	m_c'		
	500	1.25	2.35	7.189	0.219	1.320	5.623							
	1000	1.25	2.35	7.189	0.167	1.433	5.623							
$\beta = 2.6$														
$M_{cl,min}$	$\alpha_{1,IMF}$	$\alpha_{2,IMF}$	m_c	$\alpha_{1,IGIMF}$	$\alpha_{2,IGIMF}$	m_c'	$\alpha_{1,IMF}$	$\alpha_{2,IMF}$	m_c	$\alpha_{1,IGIMF}$	$\alpha_{2,IGIMF}$	m_c'		
	500	1.25	2.35	0.381	0.388	1.433	0.282	1.25	2.35	0.434	-0.404	1.400	0.224	
	1000	1.25	2.35	0.381	0.195	1.456	0.224	1.25	2.35	0.434	0.645	1.448	0.282	
$z = 0.8$														
$M_{cl,min}$	$\alpha_{1,IMF}$	$\alpha_{2,IMF}$	m_c	$\alpha_{1,IGIMF}$	$\alpha_{2,IGIMF}$	m_c'	$\alpha_{1,IMF}$	$\alpha_{2,IMF}$	m_c	$\alpha_{1,IGIMF}$	$\alpha_{2,IGIMF}$	m_c'		
	500	1.25	2.35	0.797	0.213	1.417	0.562	1.25	2.35	1.304	0.212	1.371	1.122	
	1000	1.25	2.35	0.797	-0.049	1.403	0.708	1.25	2.35	1.304	0.291	1.446	1.122	
$z = 2.2$														
$M_{cl,min}$	$\alpha_{1,IMF}$	$\alpha_{2,IMF}$	m_c	$\alpha_{1,IGIMF}$	$\alpha_{2,IGIMF}$	m_c'	$\alpha_{1,IMF}$	$\alpha_{2,IMF}$	m_c	$\alpha_{1,IGIMF}$	$\alpha_{2,IGIMF}$	m_c'		
	500	1.25	2.35	1.889	0.173	1.413	1.412	1.25	2.35	3.471	0.284	1.406	1.412	
	1000	1.25	2.35	1.889	0.298	1.394	1.412	1.25	2.35	3.471	0.221	1.333	2.818	
$z = 5.0$														
$M_{cl,min}$	$\alpha_{1,IMF}$	$\alpha_{2,IMF}$	m_c	$\alpha_{1,IGIMF}$	$\alpha_{2,IGIMF}$	m_c'	$\alpha_{1,IMF}$	$\alpha_{2,IMF}$	m_c	$\alpha_{1,IGIMF}$	$\alpha_{2,IGIMF}$	m_c'		
	500	1.25	2.35	4.849	0.218	1.412	4.467	1.25	2.35	5.981	0.241	1.385	5.623	
	1000	1.25	2.35	4.849	0.207	1.333	3.548	1.25	2.35	5.981	0.329	1.264	4.467	
$z = 6.8$														
$M_{cl,min}$	$\alpha_{1,IMF}$	$\alpha_{2,IMF}$	m_c	$\alpha_{1,IGIMF}$	$\alpha_{2,IGIMF}$	m_c'	$\alpha_{1,IMF}$	$\alpha_{2,IMF}$	m_c	$\alpha_{1,IGIMF}$	$\alpha_{2,IGIMF}$	m_c'		
	500	1.25	2.35	7.189	0.273	1.391	7.079							
	1000	1.25	2.35	7.189	0.238	1.283	7.079							

Table 4. IGIMF and IMF slopes with varying z and $M_{cl,min}$ at $\beta=2.4$ and 2.6 for SFR3:

$\beta = 2.0$													
$z = 0.1$							$z = 0.2$						
$M_{cl,min}$	$\alpha_{1,IMF}$	$\alpha_{2,IMF}$	m_c	$\alpha_{1,IGIMF}$	$\alpha_{2,IGIMF}$	$m'_{c'}$	$\alpha_{1,IMF}$	$\alpha_{2,IMF}$	m_c	$\alpha_{1,IGIMF}$	$\alpha_{2,IGIMF}$	$m'_{c'}$	
500	1.25	2.35	0.381	0.428	1.369	0.282	1.25	2.35	0.434	0.008	1.428	0.282	
1000	1.25	2.35	0.381	-0.795	1.414	0.178	1.25	2.35	0.434	-0.236	1.429	0.282	
$z = 0.8$							$z = 1.5$						
$M_{cl,min}$	$\alpha_{1,IMF}$	$\alpha_{2,IMF}$	m_c	$\alpha_{1,IGIMF}$	$\alpha_{2,IGIMF}$	$m'_{c'}$	$\alpha_{1,IMF}$	$\alpha_{2,IMF}$	m_c	$\alpha_{1,IGIMF}$	$\alpha_{2,IGIMF}$	$m'_{c'}$	
500	1.25	2.35	0.797	0.188	1.316	0.562	1.25	2.35	1.304	0.134	1.401	0.562	
1000	1.25	2.35	0.797	0.276	1.485	0.447	1.25	2.35	1.304	0.279	1.302	1.122	
$z = 2.2$							$z = 3.8$						
$M_{cl,min}$	$\alpha_{1,IMF}$	$\alpha_{2,IMF}$	m_c	$\alpha_{1,IGIMF}$	$\alpha_{2,IGIMF}$	$m'_{c'}$	$\alpha_{1,IMF}$	$\alpha_{2,IMF}$	m_c	$\alpha_{1,IGIMF}$	$\alpha_{2,IGIMF}$	$m'_{c'}$	
500	1.25	2.35	1.889	0.203	1.421	1.412	1.25	2.35	3.471	-0.117	1.232	3.548	
1000	1.25	2.35	1.889	-0.072	1.314	1.412	1.25	2.35	3.471	0.273	1.512	2.818	
$z = 5.0$							$z = 5.9$						
$M_{cl,min}$	$\alpha_{1,IMF}$	$\alpha_{2,IMF}$	m_c	$\alpha_{1,IGIMF}$	$\alpha_{2,IGIMF}$	$m'_{c'}$	$\alpha_{1,IMF}$	$\alpha_{2,IMF}$	m_c	$\alpha_{1,IGIMF}$	$\alpha_{2,IGIMF}$	$m'_{c'}$	
500	1.25	2.35	4.849	0.269	1.385	3.548	1.25	2.35	5.981	0.313	1.398	7.079	
1000	1.25	2.35	4.849	0.382	1.376	3.548	1.25	2.35	5.981	0.446	1.375	5.623	
$z = 6.8$							$z = 6.8$						
$M_{cl,min}$	$\alpha_{1,IMF}$	$\alpha_{2,IMF}$	m_c	$\alpha_{1,IGIMF}$	$\alpha_{2,IGIMF}$	$m'_{c'}$	$\alpha_{1,IMF}$	$\alpha_{2,IMF}$	m_c	$\alpha_{1,IGIMF}$	$\alpha_{2,IGIMF}$	$m'_{c'}$	
500	1.25	2.35	7.189	0.178	1.497	7.079							
1000	1.25	2.35	7.189	0.419	1.325	7.079							
$\beta = 2.4$													
$z = 0.1$							$z = 0.2$						
$M_{cl,min}$	$\alpha_{1,IMF}$	$\alpha_{2,IMF}$	m_c	$\alpha_{1,IGIMF}$	$\alpha_{2,IGIMF}$	$m'_{c'}$	$\alpha_{1,IMF}$	$\alpha_{2,IMF}$	m_c	$\alpha_{1,IGIMF}$	$\alpha_{2,IGIMF}$	$m'_{c'}$	
500	1.25	2.35	0.381	0.009	1.491	0.224	1.25	2.35	0.434	0.343	1.393	0.282	
1000	1.25	2.35	0.381	0.395	1.416	0.224	1.25	2.35	0.434	0.023	1.362	0.282	
$z = 0.8$							$z = 1.5$						
$M_{cl,min}$	$\alpha_{1,IMF}$	$\alpha_{2,IMF}$	m_c	$\alpha_{1,IGIMF}$	$\alpha_{2,IGIMF}$	$m'_{c'}$	$\alpha_{1,IMF}$	$\alpha_{2,IMF}$	m_c	$\alpha_{1,IGIMF}$	$\alpha_{2,IGIMF}$	$m'_{c'}$	
500	1.25	2.35	0.797	0.315	1.349	0.447	1.25	2.35	1.304	0.226	1.386	0.708	
1000	1.25	2.35	0.797	0.321	1.407	0.562	1.25	2.35	1.304	0.133	1.501	1.122	
$z = 2.2$							$z = 3.8$						
$M_{cl,min}$	$\alpha_{1,IMF}$	$\alpha_{2,IMF}$	m_c	$\alpha_{1,IGIMF}$	$\alpha_{2,IGIMF}$	$m'_{c'}$	$\alpha_{1,IMF}$	$\alpha_{2,IMF}$	m_c	$\alpha_{1,IGIMF}$	$\alpha_{2,IGIMF}$	$m'_{c'}$	
500	1.25	2.35	1.889	0.227	1.361	1.412	1.25	2.35	3.471	0.130	1.315	2.818	
1000	1.25	2.35	1.889	0.462	1.380	1.778	1.25	2.35	3.471	0.076	1.300	3.548	
$z = 5.0$							$z = 5.9$						
$M_{cl,min}$	$\alpha_{1,IMF}$	$\alpha_{2,IMF}$	m_c	$\alpha_{1,IGIMF}$	$\alpha_{2,IGIMF}$	$m'_{c'}$	$\alpha_{1,IMF}$	$\alpha_{2,IMF}$	m_c	$\alpha_{1,IGIMF}$	$\alpha_{2,IGIMF}$	$m'_{c'}$	
500	1.25	2.35	4.849	0.219	1.372	3.548	1.25	2.35	5.981	0.215	1.322	5.623	
1000	1.25	2.35	4.849	-0.076	1.315	4.467	1.25	2.35	5.981	0.131	1.367	5.623	
$z = 6.8$							$z = 6.8$						
$M_{cl,min}$	$\alpha_{1,IMF}$	$\alpha_{2,IMF}$	m_c	$\alpha_{1,IGIMF}$	$\alpha_{2,IGIMF}$	$m'_{c'}$	$\alpha_{1,IMF}$	$\alpha_{2,IMF}$	m_c	$\alpha_{1,IGIMF}$	$\alpha_{2,IGIMF}$	$m'_{c'}$	
500	1.25	2.35	7.189	0.337	1.420	5.623							
1000	1.25	2.35	7.189	0.268	1.349	7.079							
$\beta = 2.6$													
$z = 0.1$							$z = 0.2$						
$M_{cl,min}$	$\alpha_{1,IMF}$	$\alpha_{2,IMF}$	m_c	$\alpha_{1,IGIMF}$	$\alpha_{2,IGIMF}$	$m'_{c'}$	$\alpha_{1,IMF}$	$\alpha_{2,IMF}$	m_c	$\alpha_{1,IGIMF}$	$\alpha_{2,IGIMF}$	$m'_{c'}$	
500	1.25	2.35	0.381	-0.313	1.391	0.224	1.25	2.35	0.434	0.325	1.419	0.282	
1000	1.25	2.35	0.381	-0.017	1.393	0.224	1.25	2.35	0.434	0.052	1.500	0.282	
$z = 0.8$							$z = 1.5$						
$M_{cl,min}$	$\alpha_{1,IMF}$	$\alpha_{2,IMF}$	m_c	$\alpha_{1,IGIMF}$	$\alpha_{2,IGIMF}$	$m'_{c'}$	$\alpha_{1,IMF}$	$\alpha_{2,IMF}$	m_c	$\alpha_{1,IGIMF}$	$\alpha_{2,IGIMF}$	$m'_{c'}$	
500	1.25	2.35	0.797	0.402	1.462	0.562	1.25	2.35	1.304	0.383	1.444	0.891	
1000	1.25	2.35	0.797	0.385	1.488	0.562	1.25	2.35	1.304	0.358	1.384	0.891	
$z = 2.2$							$z = 3.8$						
$M_{cl,min}$	$\alpha_{1,IMF}$	$\alpha_{2,IMF}$	m_c	$\alpha_{1,IGIMF}$	$\alpha_{2,IGIMF}$	$m'_{c'}$	$\alpha_{1,IMF}$	$\alpha_{2,IMF}$	m_c	$\alpha_{1,IGIMF}$	$\alpha_{2,IGIMF}$	$m'_{c'}$	
500	1.25	2.35	1.889	0.246	1.366	1.412	1.25	2.35	3.471	0.266	1.328	2.818	
1000	1.25	2.35	1.889	0.307	1.370	0.891	1.25	2.35	3.471	0.294	1.426	2.818	
$z = 5.0$							$z = 5.9$						
$M_{cl,min}$	$\alpha_{1,IMF}$	$\alpha_{2,IMF}$	m_c	$\alpha_{1,IGIMF}$	$\alpha_{2,IGIMF}$	$m'_{c'}$	$\alpha_{1,IMF}$	$\alpha_{2,IMF}$	m_c	$\alpha_{1,IGIMF}$	$\alpha_{2,IGIMF}$	$m'_{c'}$	
500	1.25	2.35	4.849	0.337	1.342	4.467	1.25	2.35	5.981	0.295	1.351	5.623	
1000	1.25	2.35	4.849	0.258	1.351	3.548	1.25	2.35	5.981	0.306	1.409	5.623	
$z = 6.8$							$z = 6.8$						
$M_{cl,min}$	$\alpha_{1,IMF}$	$\alpha_{2,IMF}$	m_c	$\alpha_{1,IGIMF}$	$\alpha_{2,IGIMF}$	$m'_{c'}$	$\alpha_{1,IMF}$	$\alpha_{2,IMF}$	m_c	$\alpha_{1,IGIMF}$	$\alpha_{2,IGIMF}$	$m'_{c'}$	
500	1.25	2.35	7.189	0.279	1.381	5.623							
1000	1.25	2.35	7.189	0.187	1.506	7.079							

Table 5. IGIMF and IMF slopes with varying z and $M_{cl,min}$ at
 $\beta=2.4$ and 2.6 for SFR^* :

$\beta = 2.0$												
$z = 0.1$												
$M_{cl,min}$	$\alpha_{1,IMF}$	$\alpha_{2,IMF}$	m_c	$\alpha_{1,IGIMF}$	$\alpha_{2,IGIMF}$	m_c'	$\alpha_{1,IMF}$	$\alpha_{2,IMF}$	m_c	$\alpha_{1,IGIMF}$	$\alpha_{2,IGIMF}$	m_c'
500	1.25	2.35	0.381	-0.265	1.478	0.224	1.25	2.35	0.434	0.532	1.371	0.224
1000	1.25	2.35	0.381	0.644	1.375	0.224	1.25	2.35	0.434	0.354	1.362	0.224
$z = 0.8$												
$M_{cl,min}$	$\alpha_{1,IMF}$	$\alpha_{2,IMF}$	m_c	$\alpha_{1,IGIMF}$	$\alpha_{2,IGIMF}$	m_c'	$\alpha_{1,IMF}$	$\alpha_{2,IMF}$	m_c	$\alpha_{1,IGIMF}$	$\alpha_{2,IGIMF}$	m_c'
500	1.25	2.35	0.797	0.050	1.502	0.708	1.25	2.35	1.304	0.055	1.448	0.891
1000	1.25	2.35	0.797	0.494	1.449	0.708	1.25	2.35	1.304	0.093	1.242	0.891
$z = 2.2$												
$M_{cl,min}$	$\alpha_{1,IMF}$	$\alpha_{2,IMF}$	m_c	$\alpha_{1,IGIMF}$	$\alpha_{2,IGIMF}$	m_c'	$\alpha_{1,IMF}$	$\alpha_{2,IMF}$	m_c	$\alpha_{1,IGIMF}$	$\alpha_{2,IGIMF}$	m_c'
500	1.25	2.35	1.889	0.021	1.527	1.778	1.25	2.35	3.471	0.121	1.368	1.778
1000	1.25	2.35	1.889	0.256	1.465	1.412	1.25	2.35	3.471	0.318	1.395	2.239
$z = 5.0$												
$M_{cl,min}$	$\alpha_{1,IMF}$	$\alpha_{2,IMF}$	m_c	$\alpha_{1,IGIMF}$	$\alpha_{2,IGIMF}$	m_c'	$\alpha_{1,IMF}$	$\alpha_{2,IMF}$	m_c	$\alpha_{1,IGIMF}$	$\alpha_{2,IGIMF}$	m_c'
500	1.25	2.35	4.849	0.117	1.359	4.467	1.25	2.35	5.981	0.152	1.347	4.467
1000	1.25	2.35	4.849	0.472	1.335	4.467	1.25	2.35	5.981	0.373	1.368	4.467
$z = 6.8$												
$M_{cl,min}$	$\alpha_{1,IMF}$	$\alpha_{2,IMF}$	m_c	$\alpha_{1,IGIMF}$	$\alpha_{2,IGIMF}$	m_c'	$\alpha_{1,IMF}$	$\alpha_{2,IMF}$	m_c	$\alpha_{1,IGIMF}$	$\alpha_{2,IGIMF}$	m_c'
500	1.25	2.35	7.189	0.215	1.381	7.079						
1000	1.25	2.35	7.189	0.145	1.564	7.079						
$\beta = 2.4$												
$z = 0.1$												
$M_{cl,min}$	$\alpha_{1,IMF}$	$\alpha_{2,IMF}$	m_c	$\alpha_{1,IGIMF}$	$\alpha_{2,IGIMF}$	m_c'	$\alpha_{1,IMF}$	$\alpha_{2,IMF}$	m_c	$\alpha_{1,IGIMF}$	$\alpha_{2,IGIMF}$	m_c'
500	1.25	2.35	0.381	0.115	1.474	0.224	1.25	2.35	0.434	0.439	1.409	0.282
1000	1.25	2.35	0.381	-0.037	1.415	0.224	1.25	2.35	0.434	0.529	1.363	0.282
$z = 0.8$												
$M_{cl,min}$	$\alpha_{1,IMF}$	$\alpha_{2,IMF}$	m_c	$\alpha_{1,IGIMF}$	$\alpha_{2,IGIMF}$	m_c'	$\alpha_{1,IMF}$	$\alpha_{2,IMF}$	m_c	$\alpha_{1,IGIMF}$	$\alpha_{2,IGIMF}$	m_c'
500	1.25	2.35	0.797	0.221	1.448	0.447	1.25	2.35	1.304	0.331	1.381	0.891
1000	1.25	2.35	0.797	0.076	1.412	0.562	1.25	2.35	1.304	0.218	1.446	0.891
$z = 2.2$												
$M_{cl,min}$	$\alpha_{1,IMF}$	$\alpha_{2,IMF}$	m_c	$\alpha_{1,IGIMF}$	$\alpha_{2,IGIMF}$	m_c'	$\alpha_{1,IMF}$	$\alpha_{2,IMF}$	m_c	$\alpha_{1,IGIMF}$	$\alpha_{2,IGIMF}$	m_c'
500	1.25	2.35	1.889	0.135	1.307	1.778	1.25	2.35	3.471	0.210	1.340	2.818
1000	1.25	2.35	1.889	0.329	1.332	1.412	1.25	2.35	3.471	0.191	1.412	3.548
$z = 5.0$												
$M_{cl,min}$	$\alpha_{1,IMF}$	$\alpha_{2,IMF}$	m_c	$\alpha_{1,IGIMF}$	$\alpha_{2,IGIMF}$	m_c'	$\alpha_{1,IMF}$	$\alpha_{2,IMF}$	m_c	$\alpha_{1,IGIMF}$	$\alpha_{2,IGIMF}$	m_c'
500	1.25	2.35	4.849	0.226	1.392	4.467	1.25	2.35	5.981	-0.022	1.339	4.467
1000	1.25	2.35	4.849	0.281	1.274	4.467	1.25	2.35	5.981	0.149	1.329	4.467
$z = 6.8$												
$M_{cl,min}$	$\alpha_{1,IMF}$	$\alpha_{2,IMF}$	m_c	$\alpha_{1,IGIMF}$	$\alpha_{2,IGIMF}$	m_c'	$\alpha_{1,IMF}$	$\alpha_{2,IMF}$	m_c	$\alpha_{1,IGIMF}$	$\alpha_{2,IGIMF}$	m_c'
500	1.25	2.35	7.189	0.330	1.373	7.079						
1000	1.25	2.35	7.189	0.234	1.342	5.623						
$\beta = 2.6$												
$z = 0.1$												
$M_{cl,min}$	$\alpha_{1,IMF}$	$\alpha_{2,IMF}$	m_c	$\alpha_{1,IGIMF}$	$\alpha_{2,IGIMF}$	m_c'	$\alpha_{1,IMF}$	$\alpha_{2,IMF}$	m_c	$\alpha_{1,IGIMF}$	$\alpha_{2,IGIMF}$	m_c'
500	1.25	2.35	0.381	0.150	1.442	0.224	1.25	2.35	0.434	0.241	1.416	0.282
1000	1.25	2.35	0.381	0.211	1.416	0.224	1.25	2.35	0.434	0.240	1.418	0.282
$z = 0.8$												
$M_{cl,min}$	$\alpha_{1,IMF}$	$\alpha_{2,IMF}$	m_c	$\alpha_{1,IGIMF}$	$\alpha_{2,IGIMF}$	m_c'	$\alpha_{1,IMF}$	$\alpha_{2,IMF}$	m_c	$\alpha_{1,IGIMF}$	$\alpha_{2,IGIMF}$	m_c'
500	1.25	2.35	0.797	0.156	1.412	0.562	1.25	2.35	1.304	0.196	1.370	0.891
1000	1.25	2.35	0.797	0.260	1.426	0.562	1.25	2.35	1.304	0.224	1.463	1.122
$z = 2.2$												
$M_{cl,min}$	$\alpha_{1,IMF}$	$\alpha_{2,IMF}$	m_c	$\alpha_{1,IGIMF}$	$\alpha_{2,IGIMF}$	m_c'	$\alpha_{1,IMF}$	$\alpha_{2,IMF}$	m_c	$\alpha_{1,IGIMF}$	$\alpha_{2,IGIMF}$	m_c'
500	1.25	2.35	1.889	0.366	1.378	1.412	1.25	2.35	3.471	0.238	1.484	3.548
1000	1.25	2.35	1.889	0.295	1.487	1.412	1.25	2.35	3.471	0.276	1.261	2.818
$z = 5.0$												
$M_{cl,min}$	$\alpha_{1,IMF}$	$\alpha_{2,IMF}$	m_c	$\alpha_{1,IGIMF}$	$\alpha_{2,IGIMF}$	m_c'	$\alpha_{1,IMF}$	$\alpha_{2,IMF}$	m_c	$\alpha_{1,IGIMF}$	$\alpha_{2,IGIMF}$	m_c'
500	1.25	2.35	4.849	0.319	1.258	4.467	1.25	2.35	5.981	0.299	1.339	4.467
1000	1.25	2.35	4.849	0.344	1.523	5.623	1.25	2.35	5.981	0.314	1.281	5.623
$z = 6.8$												
$M_{cl,min}$	$\alpha_{1,IMF}$	$\alpha_{2,IMF}$	m_c	$\alpha_{1,IGIMF}$	$\alpha_{2,IGIMF}$	m_c'	$\alpha_{1,IMF}$	$\alpha_{2,IMF}$	m_c	$\alpha_{1,IGIMF}$	$\alpha_{2,IGIMF}$	m_c'
500	1.25	2.35	7.189	0.158	1.512	7.079						
1000	1.25	2.35	7.189	0.192	1.402	7.079						

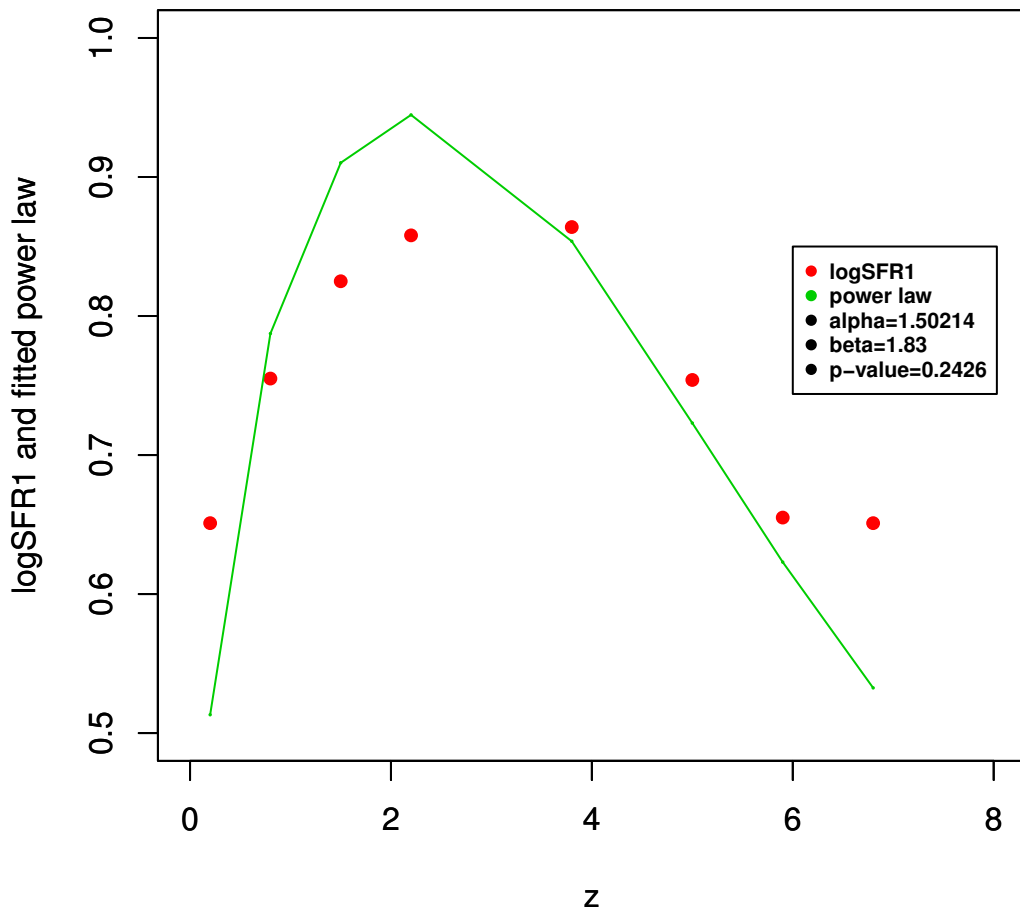


Figure 1. Tapered power law fit to the observed SFR1 as $\log_{10}(SFR1) = 10.0333 * (z^{-1.5021}) * (1 - \exp(-z/3.8)^{1.83})$, p-value = 0.2426

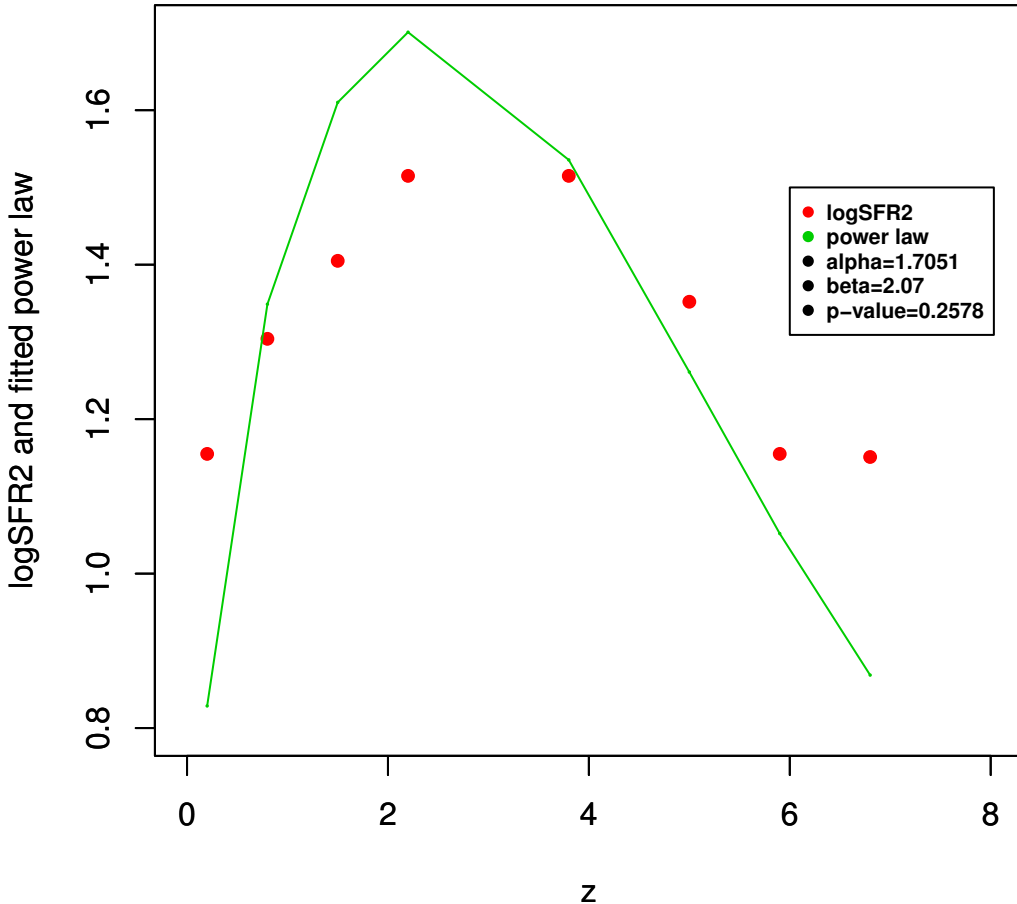


Figure 2. Tapered power law fit to the observed SFR2 as $\log_{10}(SFR2) = 23.6636 * (z^{-1.7051}) * (1 - \exp(-(z/3.8)^{2.07}))$, p-value = 0.2578

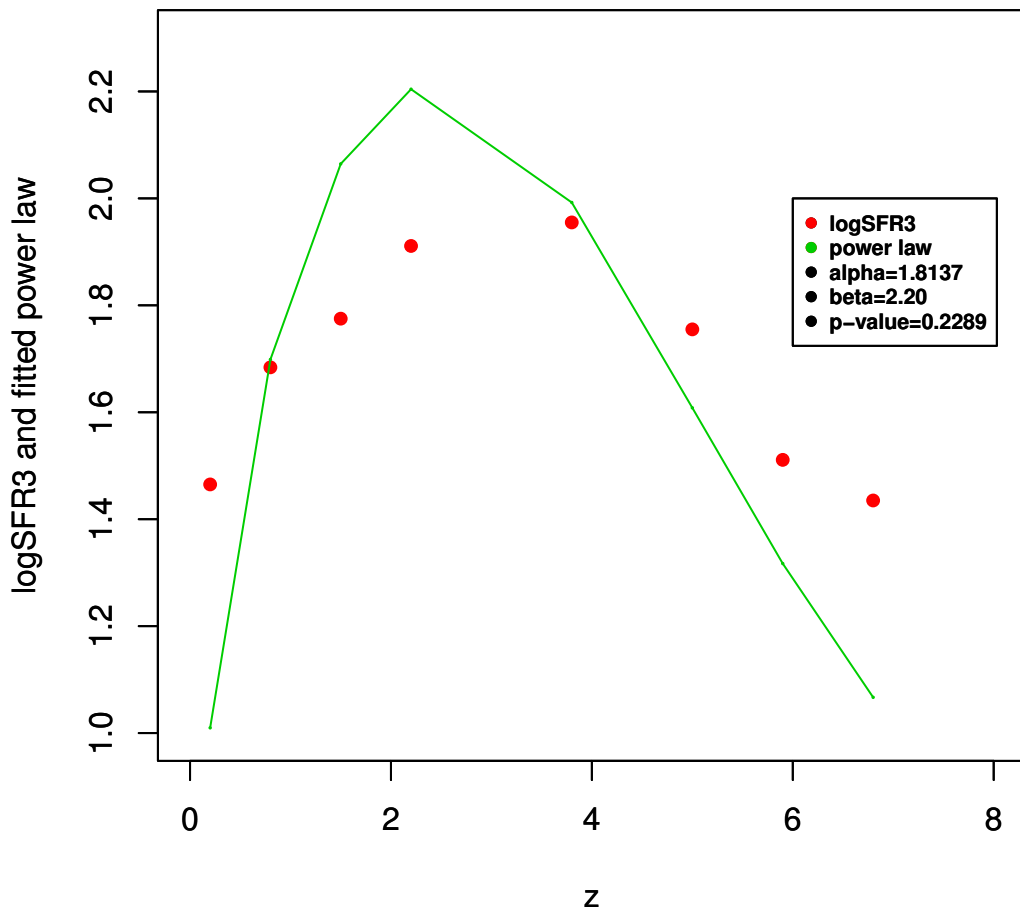


Figure 3. Tapered power law fit to the observed SFR3 as $\log_{10}(SFR3) = 35.4905 * (z^{-1.8137}) * (1 - \exp(-(z/3.8)^{2.20}))$, p-value = 0.2503

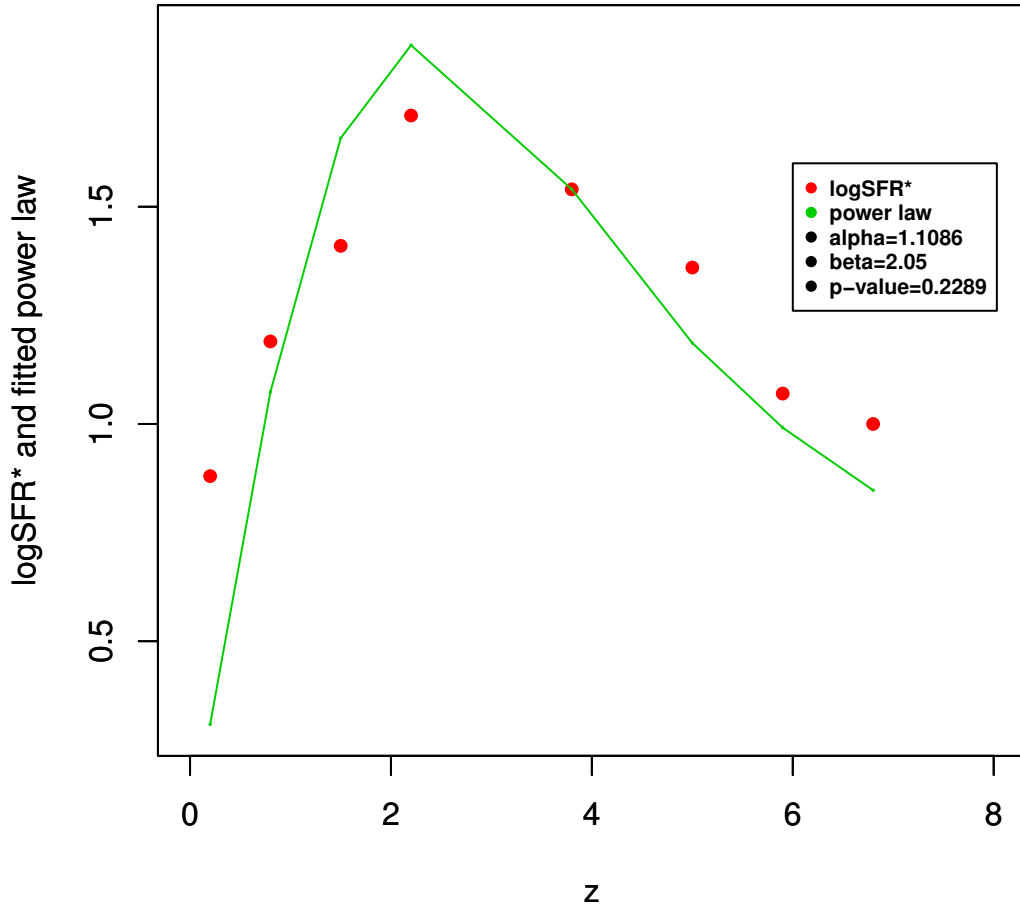


Figure 4. Tapered power law fit to the observed SFR* as $\log_{10}(SFR^*) = 7.097 * (z^{-1.1086}) * (1 - \exp(-(z/2.2)^{2.05}))$, p-value = 0.2289.

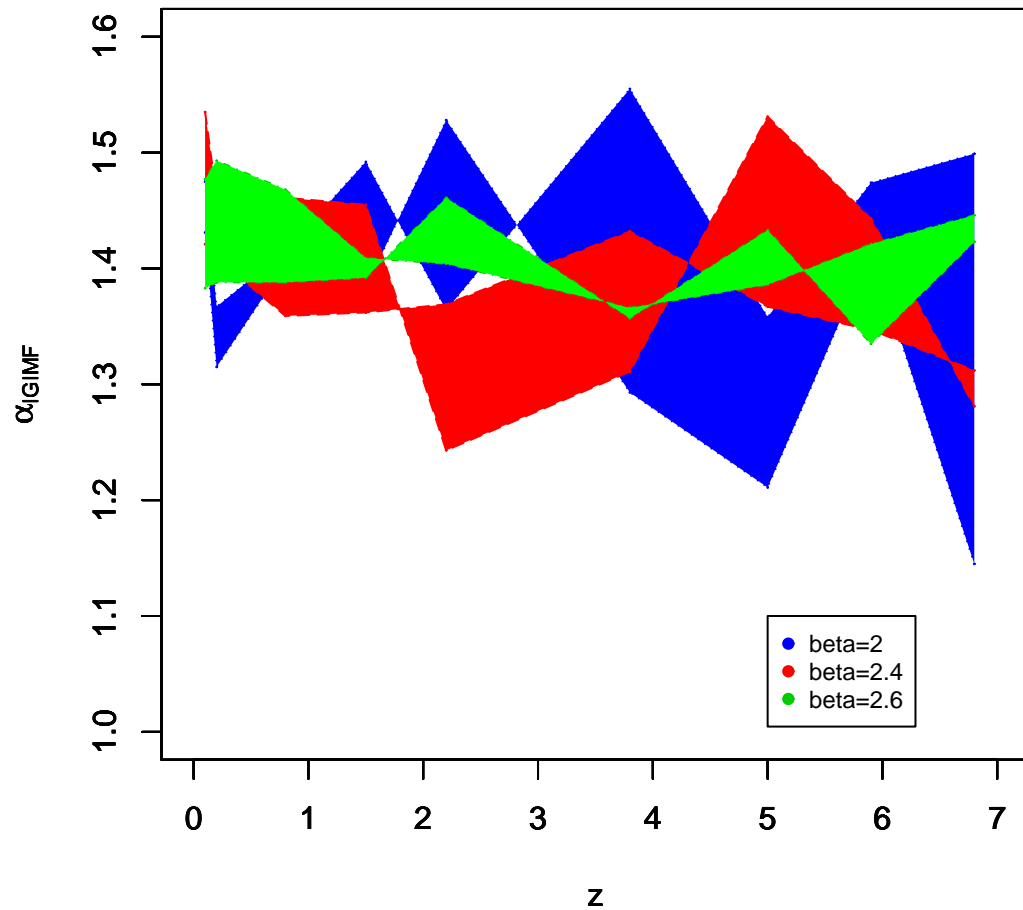


Figure 5. $\alpha_{2,IGIMF}$ as a function of z for all values of parameters given in Table 2 for SFR1 and $\beta = 2.6$ (green region), $\beta = 2.4$ (red region), $\beta = 2$ (blue region).

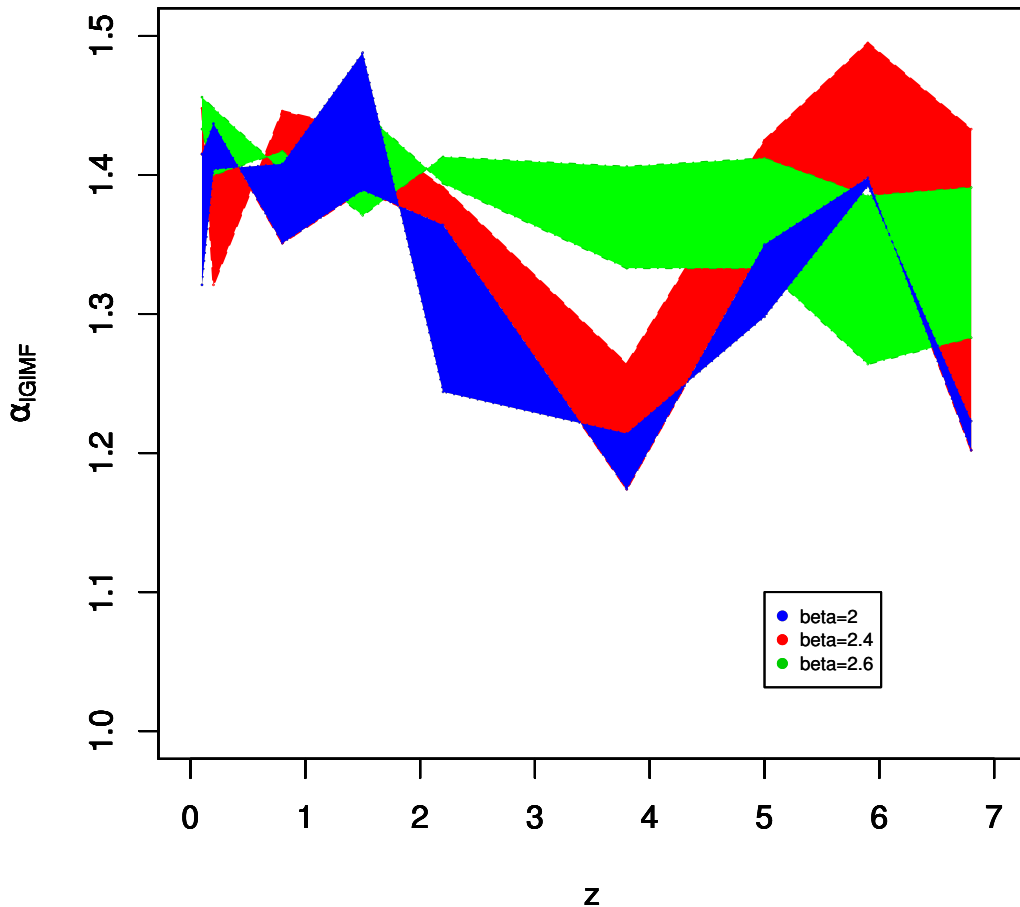


Figure 6. $\alpha_{2,IGIMF}$ as a function of z for all values of parameters given in Table 3 for SFR2 and $\beta = 2.6$ (green region), $\beta = 2.4$ (red region), $\beta = 2$ (blue region).

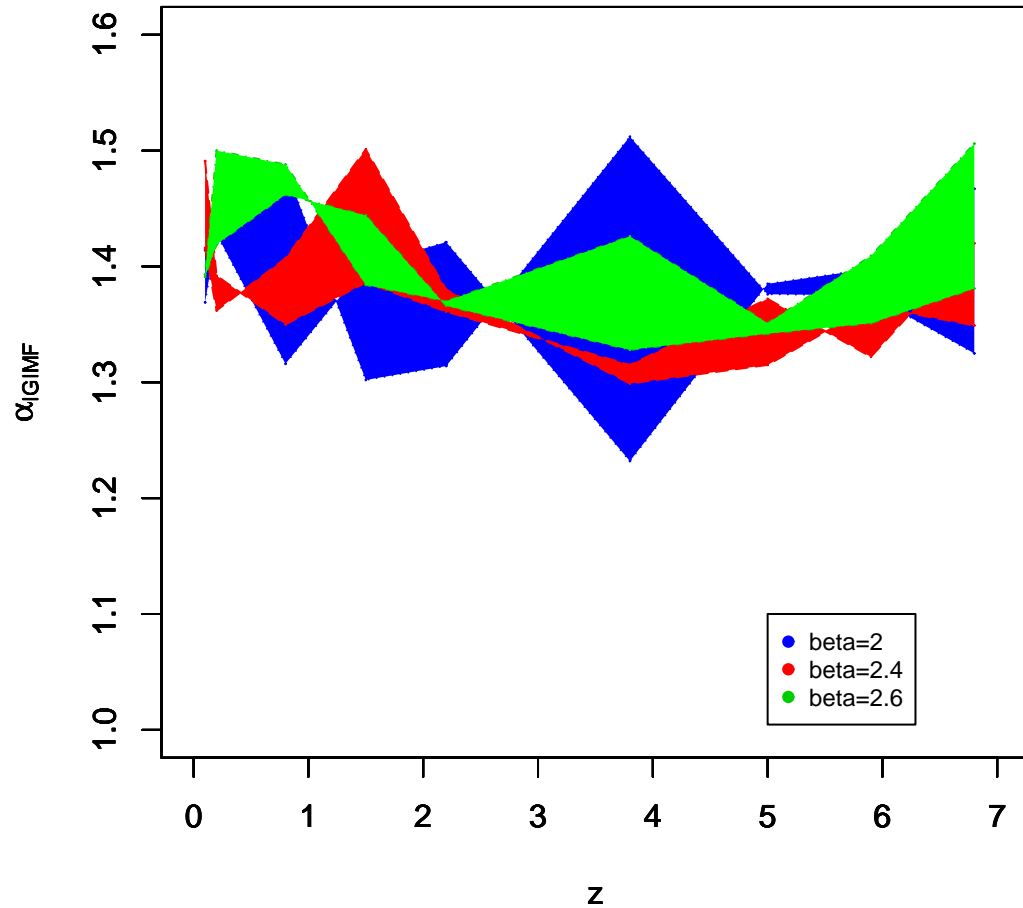


Figure 7. $\alpha_{2,IGIMF}$ as a function of z for all values of parameters given in Table 4 for SFR3 and $\beta = 2.6$ (green region), $\beta = 2.4$ (red region), $\beta = 2$ (blue region).

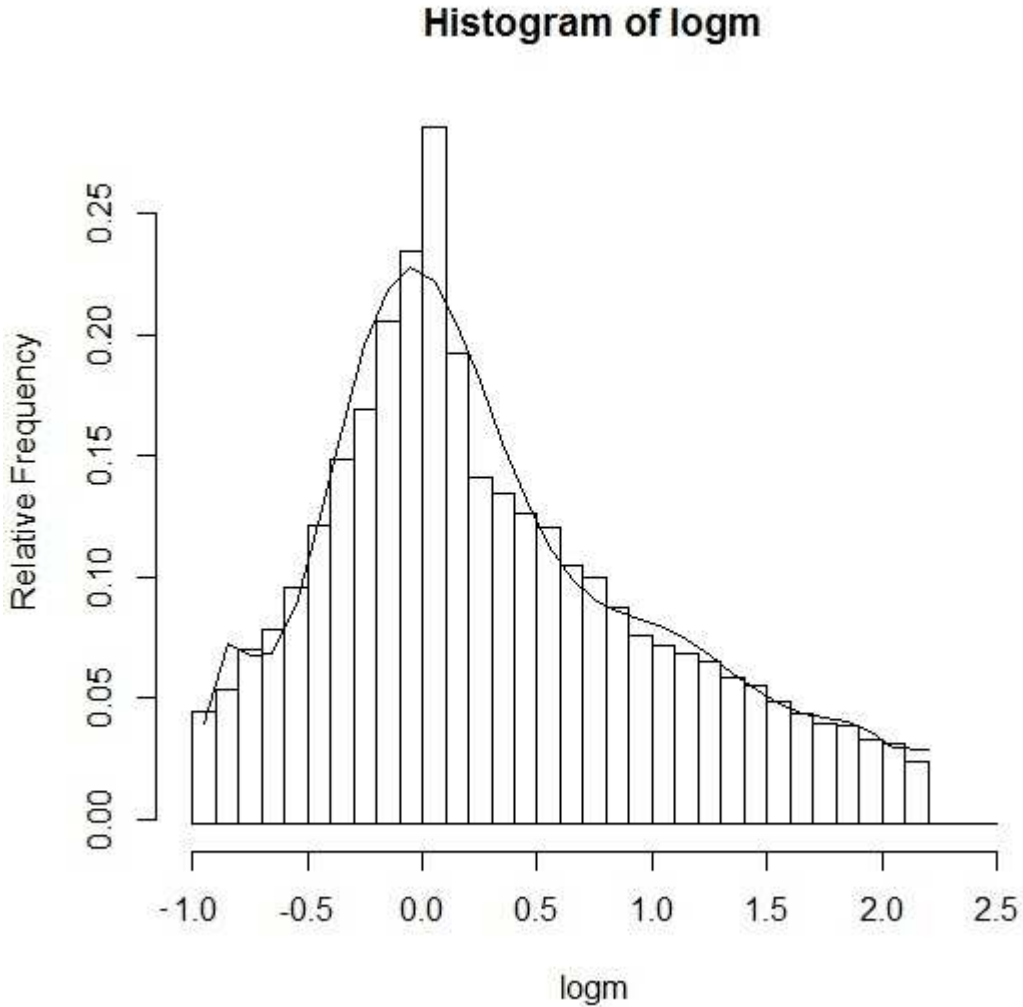


Figure 8. One representative histogram with fitted curve for the simulated points of the IGIMF ($\xi(m) = \frac{dN}{d\log m}$) for redshift $z = 1.5$, $\beta = 2$, $M_{cl, min} = 500M_\odot$ and SFR2.

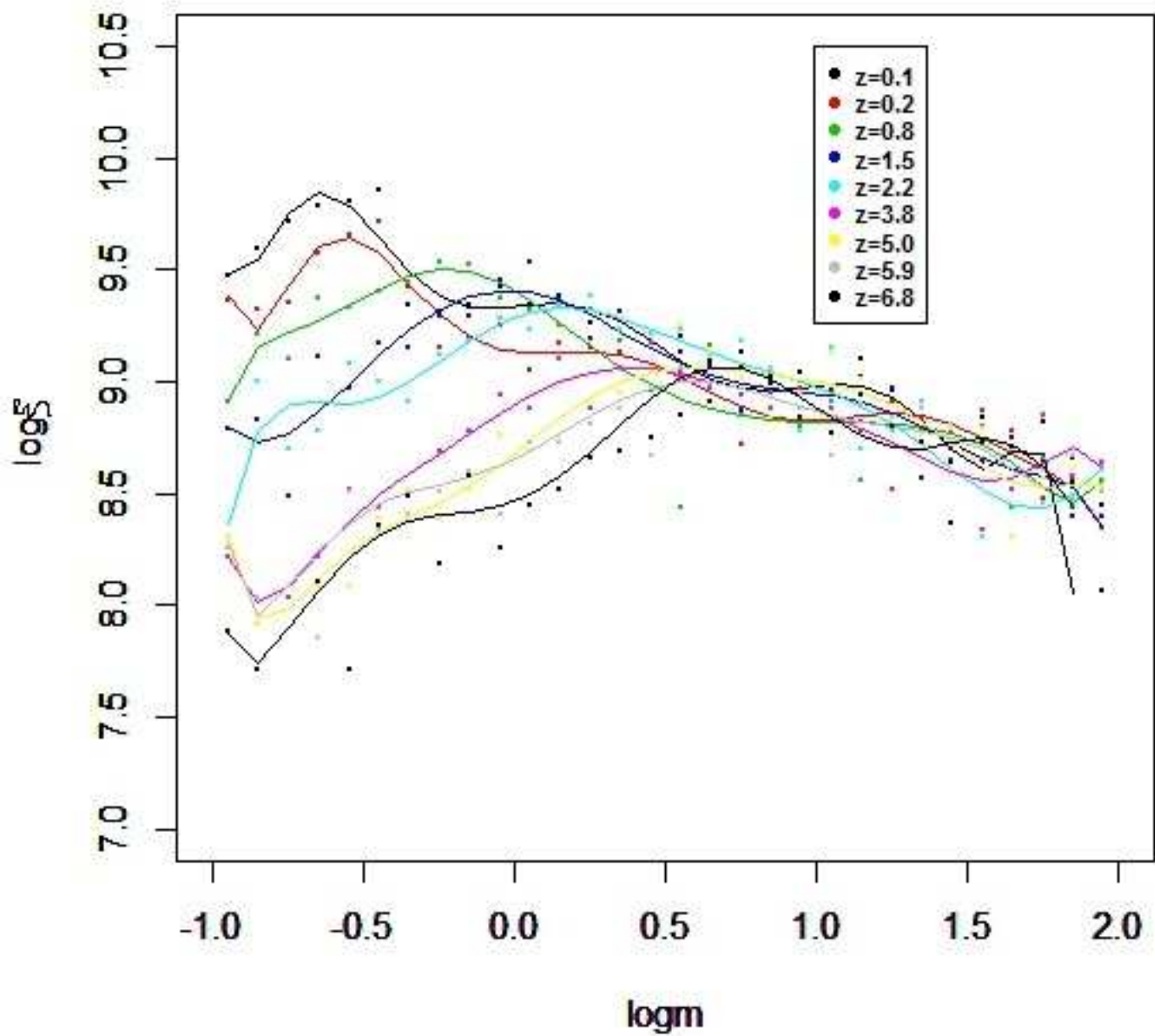


Figure 9. Fitted curves for the simulated points of the IGIMF ($\xi(m) = \frac{dN}{d\log m}$) vs $\log m$ for various redshifts at $\beta = 2$ for $M_{\text{cl}, \min} = 500M_{\odot}$ and SFR1.

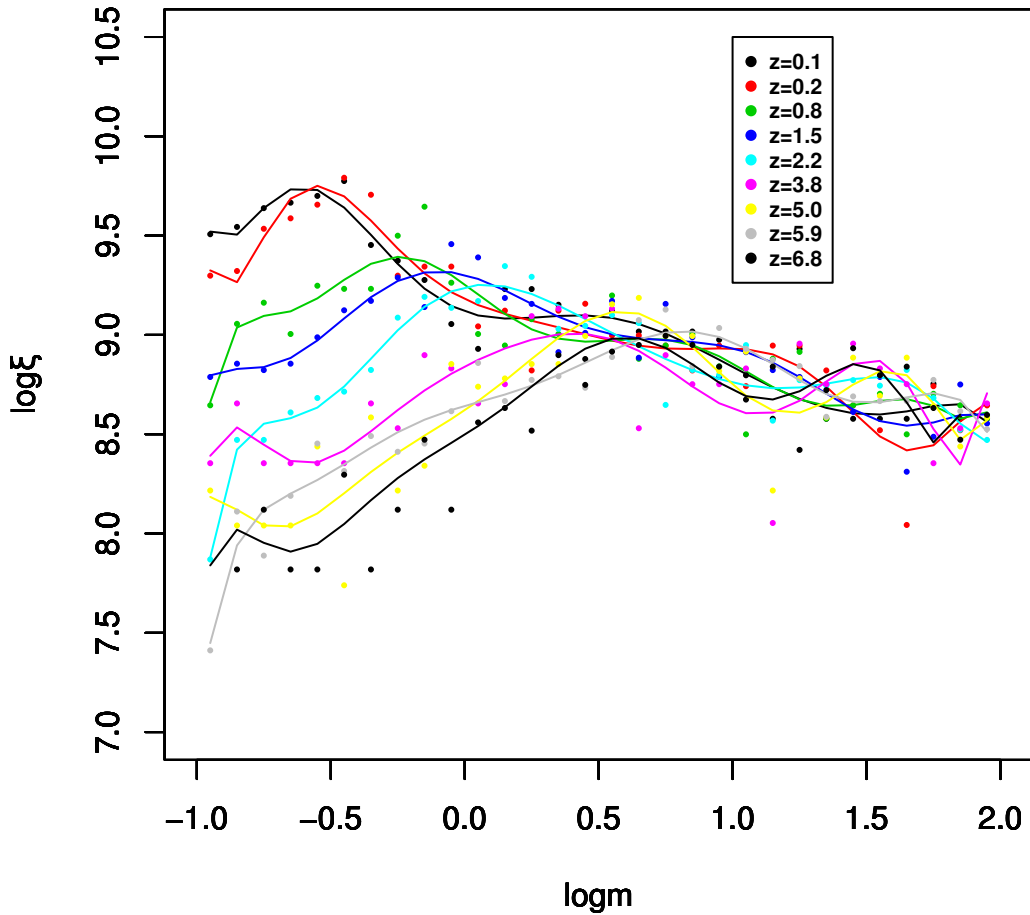


Figure 10. Fitted curves for the simulated points of the IGIMF ($\xi(m) = \frac{dN}{d\log m}$) vs $\log m$ for various redshifts at $\beta = 2$ for $M_{\text{cl,min}} = 500M_{\odot}$ and SFR2.

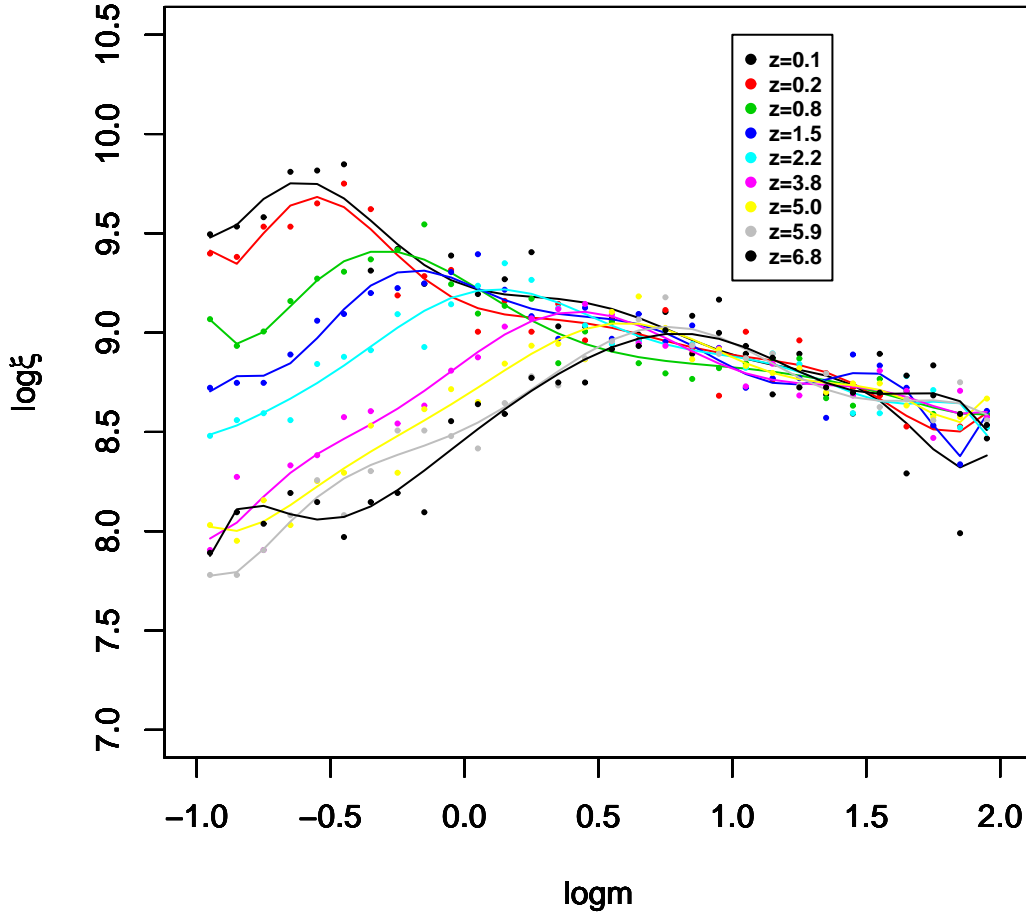


Figure 11. Fitted curves for the simulated points of the IGIMF ($\xi(m) = \frac{dN}{d\log m}$) vs $\log m$ for various redshifts at $\beta = 2$ for $M_{\text{cl}, \min} = 500 M_{\odot}$ and SFR3.

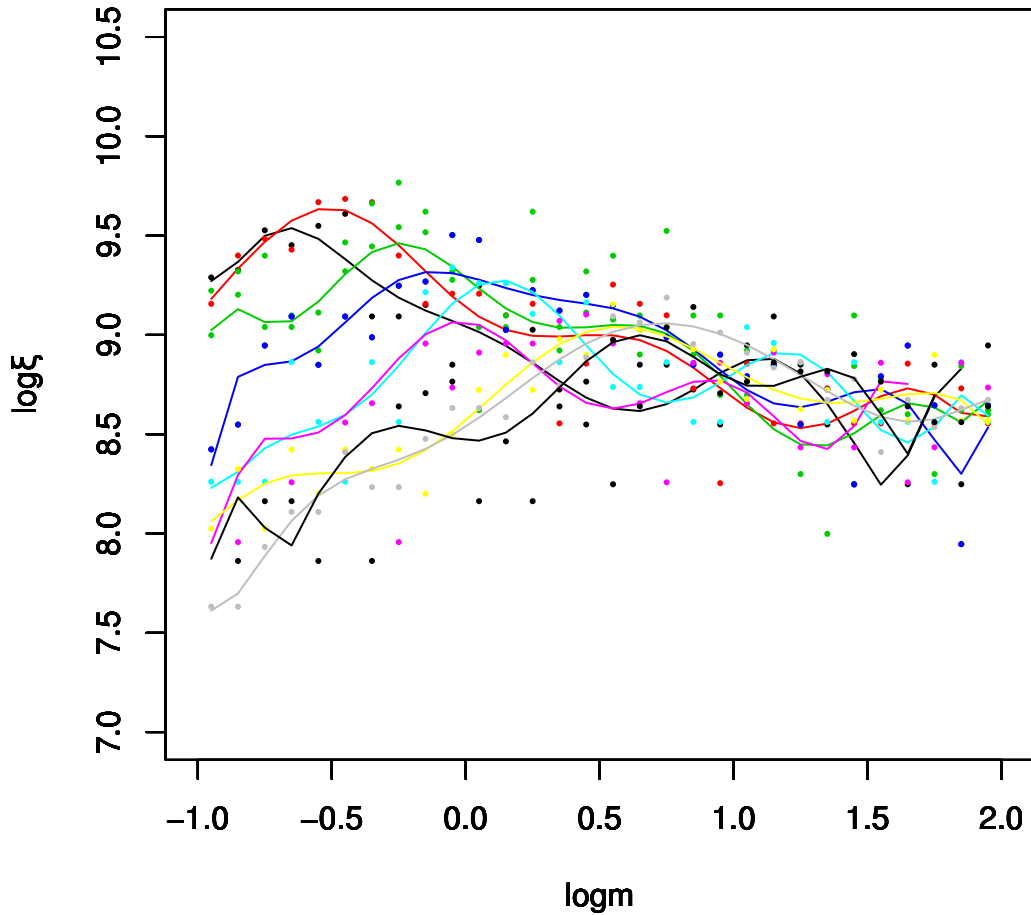


Figure 12. Fitted curves for the simulated points of the IGIMF ($\xi(m) = \frac{dN}{d\log m}$) vs $\log m$ for various redshifts at $\beta = 2$ for $M_{\text{cl}, \min} = 1000 M_{\odot}$ and SFR2.

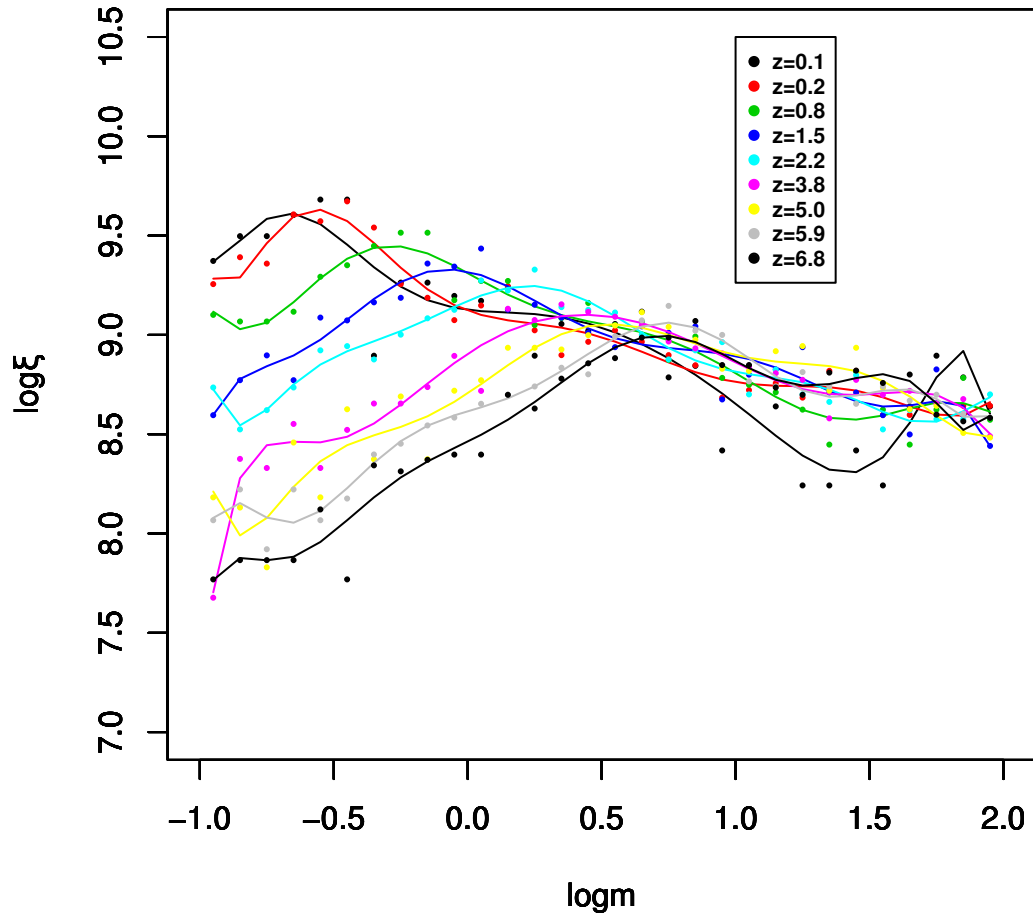


Figure 13. Fitted curves for the simulated points of the IGIMF ($\xi(m) = \frac{dN}{d\log m}$) vs $\log m$ for various redshifts at $\beta=2.4$ for $M_{\text{cl,min}} = 500 M_{\odot}$ and SFR2.

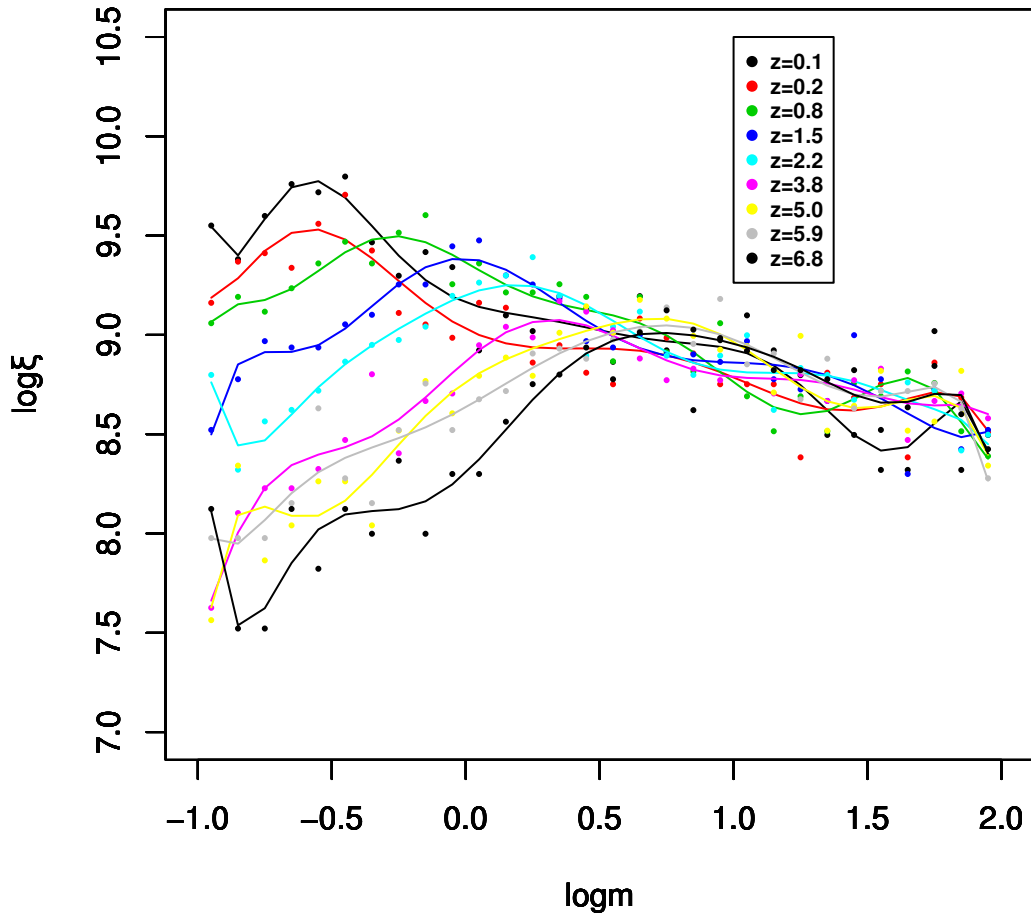


Figure 14. Fitted curves for the simulated points of the IGIMF ($\xi(m) = \frac{dN}{d\log m}$) vs $\log m$ for various redshifts at $\beta=2.4$ for $M_{\text{cl,min}} = 1000 M_\odot$ and SFR2.

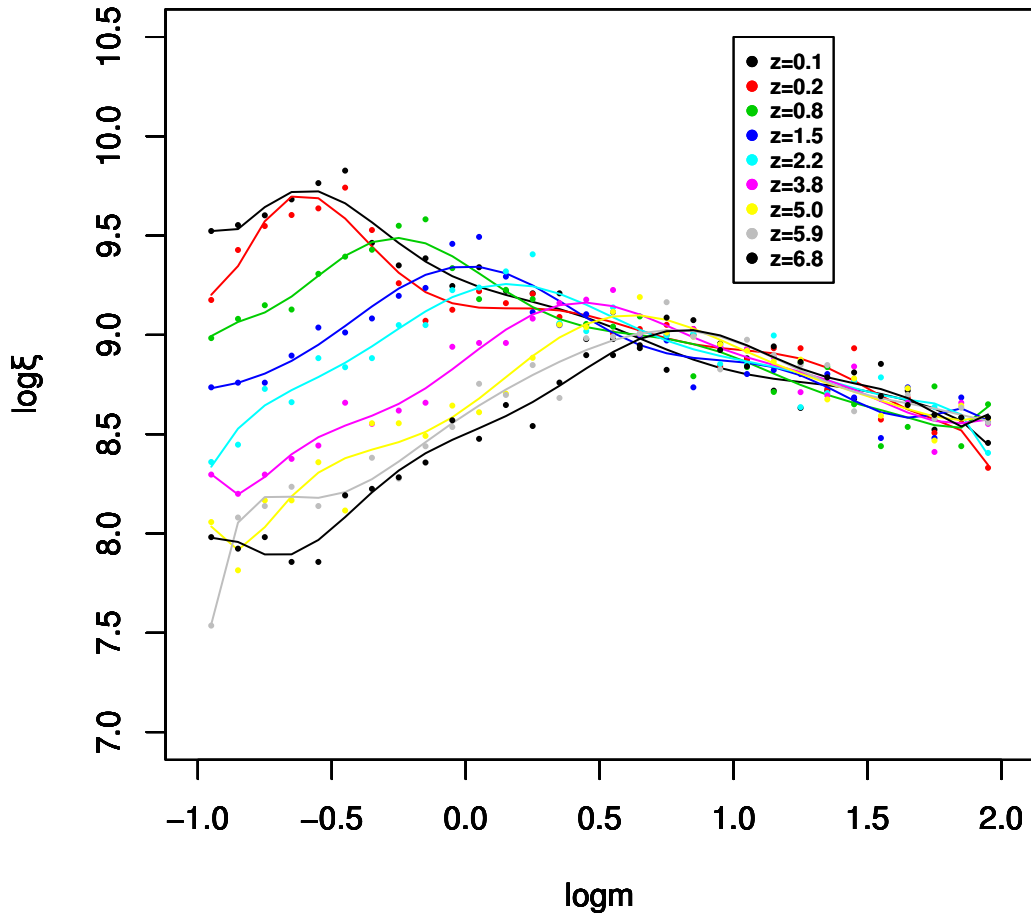


Figure 15. Fitted curves for the simulated points of the IGIMF ($\xi(m) = \frac{dN}{d\log m}$) vs $\log m$ for various redshifts at $\beta=2.6$ for $M_{\text{cl,min}} = 500 M_{\odot}$ and SFR2.

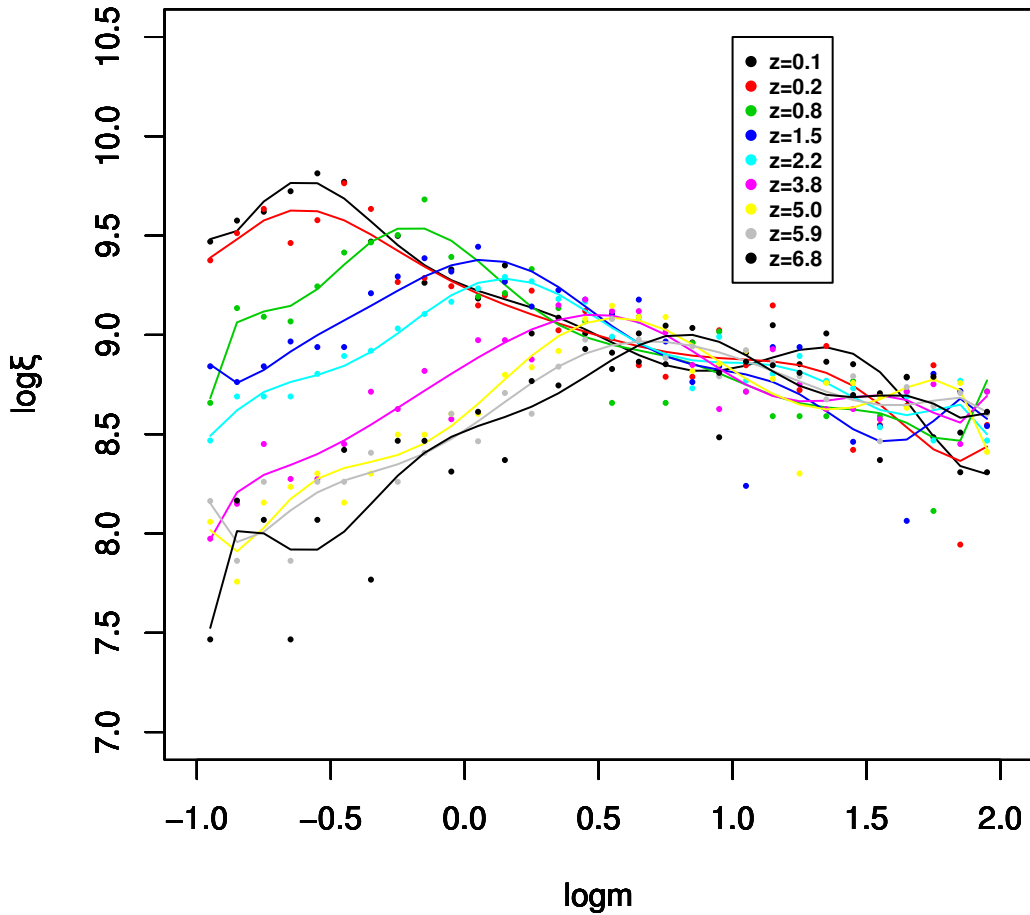


Figure 16. Fitted curves for the simulated points of the IGIMF ($\xi(m) = \frac{dN}{d\log m}$) vs $\log m$ for various redshifts at $\beta=2.6$ for $M_{\text{cl,min}} = 1000 M_{\odot}$ and SFR2